Western University
Scholarship@Western

Electronic Thesis and Dissertation Repository

4-22-2024 9:45 AM

Upgrading of Vapors and Gases from Pyrolysis to Valued Added Gaseous Products

Ivan Santiago, *Western University*

Supervisor: Franco Berruti, *The University of Western Ontario*
A thesis submitted in partial fulfillment of the requirements for the Master of Engineering
Science degree in Chemical and Biochemical Engineering
© Ivan Santiago 2024

Follow this and additional works at: https://ir.lib.uwo.ca/etd

Part of the Biochemical and Biomolecular Engineering Commons, Other Chemical Engineering Commons, and the Thermodynamics Commons

Recommended Citation

Abstract

This MSc thesis explores biomass pyrolysis and reforming, aiming to convert biomass-derived vapors into useful gases for synthesis and fuel. The study focuses on transforming high molecular weight molecules, like polycyclic aromatic hydrocarbons, and volatile organic molecules such as acids, alcohols, and other substances formed during pyrolysis into essential gases like hydrogen, methane, carbon monoxide, and carbon dioxide.

A dual-reactor system is employed: a CSTR for primary pyrolysis, followed by a PFR or PBR for secondary catalytic processing. Olivine is used as the catalyst.

The research compares three gas upgrading methods: thermal cracking, catalytic cracking, and catalytic steaming (reforming).

Results indicate that the use of olivine as a catalyst in dry and steam reforming leads to a significant increase in hydrogen and carbon monoxide production, with hydrogen yields reaching up to 40% and carbon monoxide up to 35% in the gas mixture. In comparison, thermal cracking resulted in lower hydrogen yields of around 20% and higher methane content.

Further analysis shows that catalytic reforming significantly reduces the presence of oxygenated compounds like acids and alcohols by up to 90%, improving the overall gas quality.

Keywords

Olivine, pyrolysis, thermal cracking, catalytic cracking, catalytic steaming, steam reforming, dry reforming, tar cracking.

Summary for Lay Audience.

This study investigates how to convert biomass, like plant material and organic waste, into useful gases for fuel and other valuable products. It focuses on transforming vapors produced from heated biomass into gases using olivine, a naturally occurring mineral chosen for its strength, affordability, and wide availability.

The research uses two reactors: the first heats the biomass to produce biochar (solid) and vapor; the second treats the vapor to convert it into gases. The olivine catalyst is specially prepared by heating and chemical treatment to enhance its effectiveness. The study compares different methods to find the best way to convert vapors, which include complex molecules such as acids, alcohols, and other organic substances, into useful gases.

Results show that olivine is effective in removing unwanted compounds and converting carbon dioxide into valuable gases like hydrogen and carbon monoxide. However, it is less effective in converting methane. Despite this, olivine resists carbon build-up, making it a durable and reliable choice for this process.

Overall, this study helps improve the process of turning biomass into energy and valuable products, contributing to more efficient and sustainable energy production methods.

Dedicatory

Dedicated to God in His expression as an infinite universe, providing me with an unparalleled mother, a special father, a supportive family, and very good friends.

Acknowledgements

Table of contents

List of tables

List of figures

Nomenclature

AR: As received.

CSTR: Continuous stirred tank reactor.

CC: Catalytic cracking.

CS: Catalytic steaming.

DB: Dry basis.

DAF: Dry ash free basis.

GC-MS: Gas chromatography-mass spectrometry.

HCR: Hydrogen consumption ratio.

HHV: High heating value.

HPLC: High pressure liquid chromatography.

LHV: Lower heating value.

PAH: Polycyclic aromatic hydrocarbons.

PRBC: Pyrolysis baseline case.

PBR: Packed bed reactor.

PFR: Plug flow reactor.

S/C: Steam carbon ratio (mol/mol).

SEM: Scanning electron microscopy.

TC: Thermal cracking.

TCBC: Thermal cracking baseline case.

TDS: Technical data sheet.

TPR: Temperature programmed reduction.

VOC: Volatile organic compounds.

WGSR: Water gas shift reaction.

WHSV: Weight hourly space velocity.

Chapter 1

1 Introduction

1.1 Background

Biomass pyrolysis, the process of heating organic materials in the absence of oxygen to produce valuable products like gases, bio-oil, and biochar, is a promising avenue for sustainable energy production. Pyrolysis typically generates a mixture of gases including hydrogen (H_2), methane (CH_4), carbon monoxide (CO), carbon dioxide (CO_2), and various hydrocarbons, depending on the biomass feedstock and operating conditions (Azeez et al., 2010), (L. Wang et al., 2022).

In a broader sense, biomass pyrolysis is a thermochemical process that converts organic materials, such as agricultural residues, wood, and other plant-based materials, into valuable products through the application of heat in the absence of oxygen. This process decomposes the biomass into three primary products: biochar (solid), bio-oil (liquid), and syngas (gaseous mixture). Pyrolysis is considered a promising technology for the sustainable production of energy and chemicals, as it provides a means to utilize renewable resources and reduce reliance on fossil fuels.

The process of biomass pyrolysis involves heating the biomass to a specific maximum temperature, known as the pyrolysis temperature. The rate at which this temperature is reached is referred to as the heating rate. Once the pyrolysis temperature is achieved, the biomass is maintained at that temperature for a specified duration, known as the residence time. During this period, the biomass undergoes a series of complex chemical reactions, including depolymerization, fragmentation, and volatilization. These reactions break down the long-chain polymers—such as cellulose, hemicellulose, and lignin—that constitute the biomass, forming smaller molecular weight compounds.

This refined version maintains the comprehensiveness and clarity of the original description while ensuring readability.

Biomass pyrolysis can be categorized into three main types based on the operational conditions and desired products:

- ➢ Slow pyrolysis: conducted at lower temperatures (300-400°C) and longer residence times (5 - 30 min), slow pyrolysis primarily produces biochar, which can be used as a soil amendment, carbon sequestration agent, or as a precursor for activated carbon.
- ➢ Fast pyrolysis: performed at moderate temperatures (450-600°C) with short residence times (1 - 2 s) and high heating rates, fast pyrolysis aims to maximize the production of bio-oil. Bio-oil can be further refined into liquid fuels or used as a feedstock for chemical production.
- ➢ Flash pyrolysis: this method operates at high temperatures (up to 700°C) and very short residence (< 1 s) times with extremely high heating rates, yielding a higher proportion of syngas. Syngas, composed mainly of hydrogen, carbon monoxide, and methane, can be utilized for power generation or as a building block for various chemical syntheses. (Basu, 2010).

As mentioned before, the main products of the biomass pyrolysis are three:
- ➢ Solid: known as char or biochar is the solid yield of pyrolysis and its composition is primarily carbon (75% - 80%) but contains oxygen and hydrogen. Its LHV is greater than the original from biomass.
- ➢ Liquid: the liquid yield of biomass pyrolysis is formed when the gaseous fraction is cooled down condensing part of it forming the liquid yield. This liquid fraction has the name of bio-oil, tar or bio-crude, consisting of water up to 30%, complex hydrocarbons, phenolic compounds, hydroxyaldehydes, hydroxyketones, carboxylic acids, sugars, small lignin molecules, sugars, and dehydrosugars.
- ➢ Gas: the permanent gas fraction or non condensable fraction contains low-molecular-weight gases like carbon dioxide, carbon monoxide, methane, ethylene, ethane, propane, propylene, and hydrogen.

Several studies have investigated various aspects of biomass pyrolysis and subsequent reforming processes to optimize the conversion of biomass into useful products using different class of catalyst (Abou Rjeily, Chaghouri, et al., 2023), (Arregi et al., 2016).

Some of the catalyst used in the reforming process of pyrolysis and gasification demand a time-consuming preparation step, including the use of expensive metals, alloys and supports (Tomishige et al., 2004).

Olivine offers a series of advantages for use as a catalyst in gas reforming processes and as a fluidized bed in pyrolysis and gasification. Some of these properties include resistance to attrition, low cost, and excellent availability. The major producer of olivine is Norway, being mined in Swedeen, Finland, Spain, Italy, Austria, Greece, Cyprus and Balkans (Marinkovic et al., 2015).

1.2 Scope of this study

The study presented here focuses on the quantitative evaluation of olivine as a catalyst in the gas and vapor upgrading process, compared to thermal cracking without the use of a catalyst. To achieve this, the first stage involves creating a baseline pyrolysis case, which will serve as a reference point for all subsequent upgrading processes.

In Chapter 3, the baseline pyrolysis case is developed. The temperature and operating pressure of the CSTR reactor are set, and various tests are conducted with a variable feed rate. The respective yields of the three main fractions of the pyrolysis process—biochar, bio-oil, and gases—are determined. It is found that, due to the volume of the reactor, temperature control, and continuous biochar extraction, the feed rate has a very slight influence on the composition of the pyrolysis gas and the yields of the fractions. This allows for an operational range of the pyrolysis process in which compositions and yields remain constant.

After creating the baseline pyrolysis case, the gas and vapor upgrading processes are carried out under the same temperature and pressure conditions. For this upgrading process, a second reactor is used where the vapors and gases are introduced. Yields are quantified, and the composition of gases and biochar is analyzed to perform material balances, obtaining a quantitative analysis of the overall yields of the fractions.

The thermal cracking process is explained in Chapter 4 to evaluate its effect on the gas composition and yield of gases. This process is evaluated under constant operating conditions of temperature and pressure, varying the residence time.

Chapter 5 is dedicated to catalytic cracking, using olivine as a catalyst. The effectiveness of the catalyst compared to thermal cracking is evaluated under the same temperature and pressure, analyzing how the ratio of gas mass flow to catalyst charge influences the gas composition and yield.

Finally, in Chapter 6, the effect of steam injection is studied under catalytic conditions, evaluating the net effect of steam on the gas composition while keeping the catalyst.

The calcination and activation procedure of olivine is carried out based on the study of various bibliographic sources. These conditions are kept constant throughout all experimental tests to maintain a consistent reference point.

The effectiveness in removing high molecular weight aromatic substances, commonly referred to as PAHs, is measured qualitatively based on the visual appearance of the cotton filter at the end of the test. Additionally, a solvent extraction process is performed on the trapped substances to determine the similarity of the results obtained with those reported in the literature under similar operating conditions.

1.3 Objectives

➤ To develop a baseline pyrolysis case to obtain yields and compositions that will serve as a reference point.

➤ To carry out a thermal treatment to determine the effect of temperature on gas yields and composition.

➤ To study the effect of using olivine as a catalyst under the same conditions as the thermal treatment to evaluate its activity as a catalyst.

➤ To evaluate the effect of steam injection on the catalytic reforming process in terms of reducing high molecular weight aromatic substances and the net effect on Hydrogen produced in the gas stream.

Chapter 2

2 Experimental and analytical and materials and methods

2.1 Biomass characterization

The biomass used in the experimental part corresponds to a commercial form of "Wood Pellets". The information provided by the supplier is as follows: "Calorific value 8500 BTU/lb, Mixture of softwood and hardwood."

The analyses conducted in the laboratory were as follows: Proximate analysis (Volatiles, Fixed Carbon, and Ash), Moisture, and Elemental analysis (Carbon, Hydrogen, and Oxygen content).

➢ The **proximate analysis** was performed according to the ASTM E-872, for the determination of volatile matter, the ASTM D-1102 for the determination of ash. The moisture content was determined using an automatic analyzer, in this case was the METTER TOLEDO HB43-S. The fixed carbon is determined by difference from the volatiles and fixed carbon.

➢ **Elemental analysis** was conducted using the respective equipment available CHNS-O Analyzer Flash EA 1112 Series, equipped with electrolytic copper and copper oxide columns.

The results are summarized in the next tables:

Table 2-1 Biomass composition as received

Biomass composition as received. (% Mass)	
Moisture	6.54%
C	44.08%
H	5.69%
O	42.66%
Ash	1.03%

The results obtained here will mostly be reported using biomass-AR as the calculation basis, meaning including ash and moisture present at the time of processing. When deemed appropriate,

calculations will be reported on what is commonly referred to as DAF, meaning without including moisture and ash content. Therefore, the terms biomass and biomass-AR refer to the same material.

Table 2-2 Biomass composition dry basis

Biomass composition dry basis (% Mass)	
C	47.16%
H	6.09%
O	45.65%
Ash	1.10%

Table 2-3 Biomass composition dry ash free basis

Biomass composition dry ash free basis (% Mass)	
C	47.69%
H	6.16%
O	46.15%

Table 2-4 Biomass proximate analysis

Proximate analysis (% Mass)	
Volatiles	82.25%
Fixed Carbon	16.72%
Ash	1.03%

Table 2-5 Elemental distribution

Mass base (g)	100	C	H	O	Ash
Biomass DAF	92.43	44.08	5.69	42.66	0.00
Ash	1.03	0.00	0.00	0.00	1.03
Moisture	6.54	0.00	0.73	5.81	0.00
TOTAL	100.00	44.08	6.42	48.47	1.03

The table 2.5 shows the contribution of each one of the components present in the whole biomass (biomass-DAF, ash, and moisture). This table, shown graphically in the Figure 2-1 allows the total mass balance.
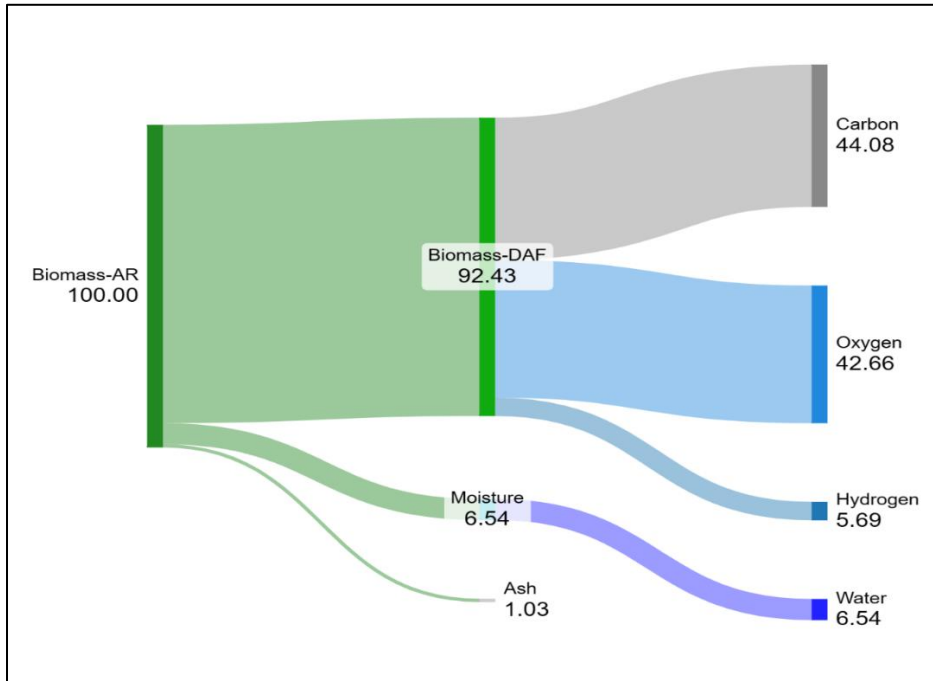
Figure 0-1 Graphical representation of elemental composition

Figure 0-2 Commercial presentation of wood pellets

The original wood pellets have a cylindrical shape with a diameter of 5 mm and a length between 5 mm and 20 mm. For the experimental part, the biomass was ground and classified to a size between 2mm and 4mm. The figures 2.3 show the original biomass and the ground.

a   **b**

Figure 0-3 a) Wood pellets as received   b) Ground biomass

The supplier reports a Calorific Value of 8500 BTU/lb, equivalent to 19.8 MJ/kg. This value has been compared with the value calculated using the correlation proposed by (Channiwala & Parikh, n.d.). In this work, the calculation of the HHV for solid, liquid, and gaseous fuels is done with the information about the elemental composition of the fuel. The correlation is given by:

$$HHV\left[{}^{MJ}/_{kg}\right] = 0.3491 * C + 1.1783 * H + 0.1005 * S - 0.1034 * O$$
$$- 0.0151 * N - 0.0211 * Ash$$

1

Where *C, H, S, O, N, Ash*, represent carbon, hydrogen, sulphur, oxygen, nitrogen, and ash contents of material, respectively, expressed in mass percentages on dry basis. Taking the values calculated in table 2.2, the HHV value for the Biomass is: 18.90 MJ/kg. The error in this value, taking the reported as the correct, is -4.56%.

2.2 Biochar composition

The elemental composition of the Biochar was made with the Elemental analyzer Flash EA 1112 Series.

2.3 Gases composition

To collect the samples of gas, Multi-layer Foil Gas Sampling Bags, Brand Restek, were used. Then, the gas collected was analyzed in the *Micro-GC Variant CP-4900 with TC Detector* equipped with Columns PPU H BF (10m), 5 CB H (8m), and M5A H BF (10m). For each of the samples, 6 analyses were conducted, discarding the first three and taking the arithmetic average of the last three as the composition value, then normalizing the concentrations to reach 100%.

2.4 Vapors (bio-oil) composition

The elemental composition of the bio-oil or vapors was calculated using the yields and composition for the biochar and gases. With this information, along with the elemental composition of the biomass and atomic mass balance considerations, the final composition of the bio-oil is determined. However, in certain instances, to confirm the presence of specific components in the final tar (condensable), as well as the species captured in the physical filter at the end of the condensing train, the following equipment was utilized for analysis: *HPLC SHIMADZU DGU-20A*, Column Agilent Technologies Hi-Plex H 300. And the *GC/MS* Agilent Technologies 7890A GC System and 5975C VL MSD with Triple-Axis Detector, Column Agilent Technologies HP-5MS.

2.5 Pyrolysis and cracking reactor

The technical description of the equipment is summarized in the next table:

Table 2-6 Reactors technical specifications

PYROLYSIS UNIT CSTR-Semi Continuous-BATCH Reactor	
Reactor total volume	1800 cm^3
Cylindrical shape ratio H/D	2/1
Electrical heating power	2000 W
Maximum operating temperature	750 ºC
CRACKING UNIT Tubular Reactor PFR - PBR	
Diameter	5.25 cm
Heated length	55.0 cm
Heated volume	1190 cm^3
Electrical heating power	7200 W
Maximum operating temperature	1100 ºC
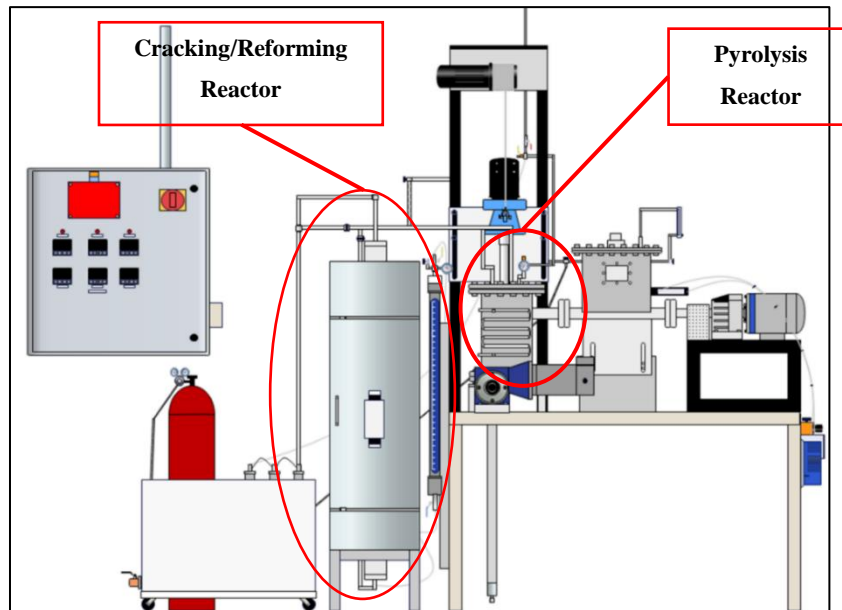
Figure 0-4 Scheme of equipment used in experimental part (Elaborated by Joshua Collen)

Figure 0-5 Photo of pyrolysis and reforming system

2.6 Olivine characterization

In this study mineral olivine is utilized as catalyst for the catalytic cracking experimental part. The mineral was supplied by SIBELCO, and its main physical properties, as reported in Table 2.7, were extracted from the respective TDS. The original olivine was classified based on its particle size, with the experimental part of this study employing the fraction with particle sizes ranging from 1.0 mm to 1.2 mm. For electron microscopy analysis, the fraction with particle sizes ranging from 180 micrometers to 250 micrometers (Sieve No 60 and No 80) was utilized.

Table 2-7 Technical specifications for olivine

Density	3.3 g/cm^3
Bulk density	1.6 – 1.9 g/cm^3
Stowage factor	0.53 – 0.63 m^3/t
Melting point	1400 – 1700 ^{o}C
CAS-No	1317-71-1
Another name	Magnesium iron Silicate
Linear Formula	$(Mg,Fe)_2SiO_4$

The TDS given by the supplier does not report a more specific chemical composition, however, in the work done by (Marinkovic et al., 2015), the same brand (SIBELCO) is used in the experimental procedure, the chemical composition is given in table 2.8.

Table 2-8 Chemical composition of olivine

MgO	49.60%
SiO$_2$	41.70%
Fe$_2$O$_3$	7.40%
Al$_2$O$_3$	0.46%
Cr$_2$O$_3$	0.31%
NiO	0.32%

The elemental composition of the original olivine was determined using SEM as analytical technique. This analysis was performed using the equipment "Hitachi SU8230 Regulus Ultra High-Resolution Field Emission SEM", available at "Surface Sciences Western". The analysis was performed to reveal the changes due to the activation or modification processes. The figure 2.6 and 2.7 reveal the composition of the original or unmodified olivine.
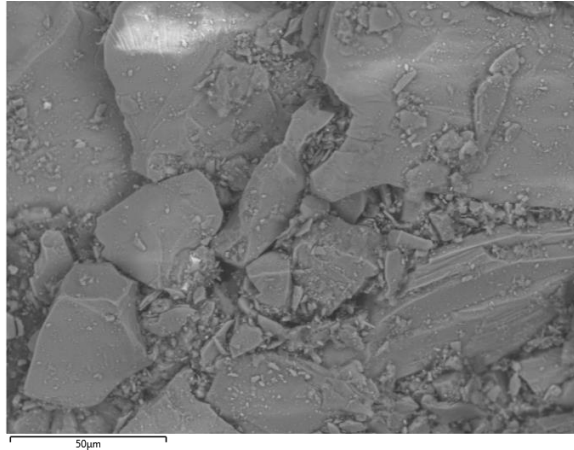
Figure 0-6 SEM for raw olivine
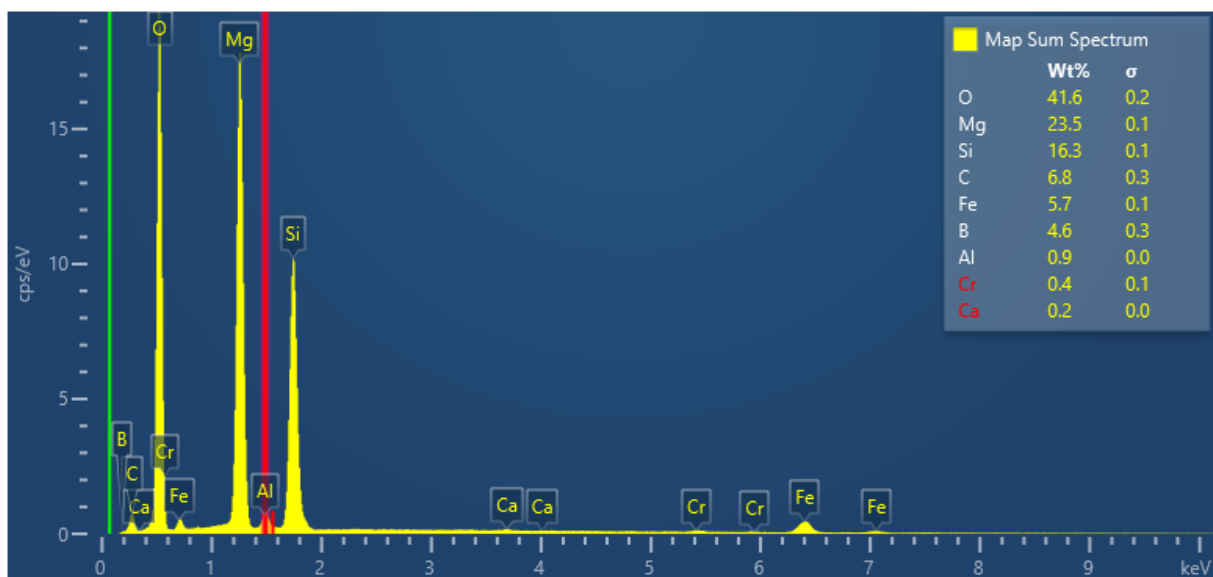
Figure 0-7 Elemental olivine composition SEM report

2.7 Experimental procedures

The experimental procedures for each of the different assays will be explained below. For all experiments, some operations are common, in special those referents to the yield calculations, which are: 1. Weighing each of the clean condensers before starting the respective assay, including the weight of the cotton filter, which is renewed in each assay. 2. Weighing the Biochar collector.

2.7.1 Olivine calcination

In the studies done by (Devi, Craje, et al., 2005), and (Devi, Ptasinski, et al., 2005), and (Fredriksson et al., 2013), the calcination of the olivine was done between 750 ºC and 900 ºC, reaching a conversion of 62% of naphthalene as tar model. Other authors are treated the olivine under different conditions, for example (Kuhn et al., 2008), used 1600 ºC as the temperature for calcination process reaching a 92% of conversion for toluene as tar substance model.

Due to limitations in Heating elements and materials resistance regarding the reactor and auxiliars equipment, the temperature for this part was set at 950 ºC, Table 2.9 summarizes the calcination operational conditions.

Table 2-9 Olivine calcination operating conditions

Heating ramp-up	8 ºC/min
Temperature (Holding)	950 ºC
Calcination time (Holding)	4 h

14

Gas	Air
Gas flow	10 Nl/min

The conditions shown in table 2.9 were the same for all the calcinations done independently of the amount of Olivine Packed inside the reactor.

The effect of calcination is illustrated by the subsequent SEM analysis.
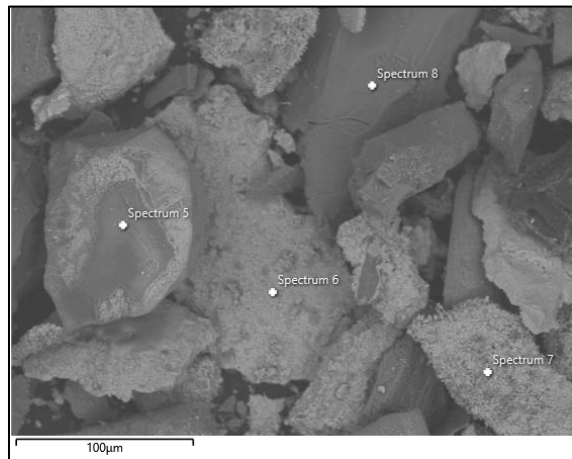
Figure 0-8 SEM for olivine calcinated
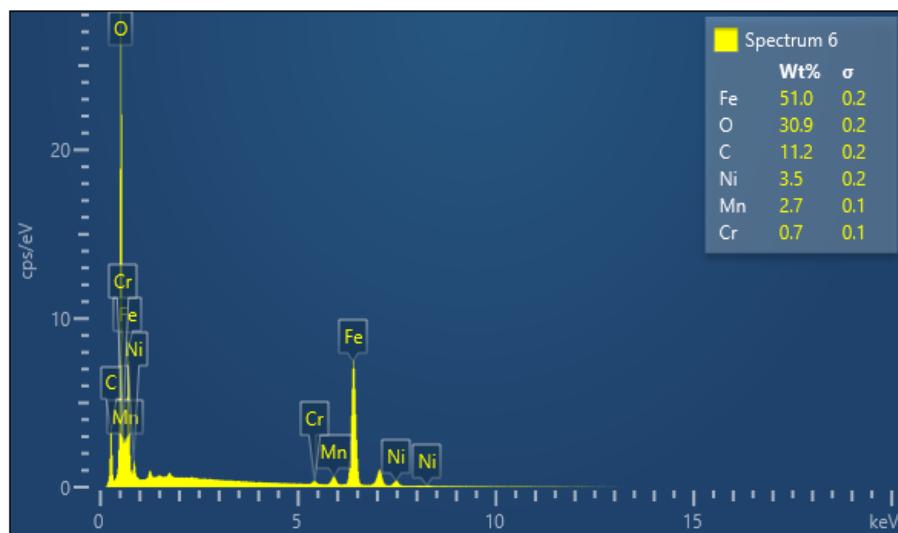
Figure 0-9 Composition of olivine calcinated in point 6 SEM figure 2.8
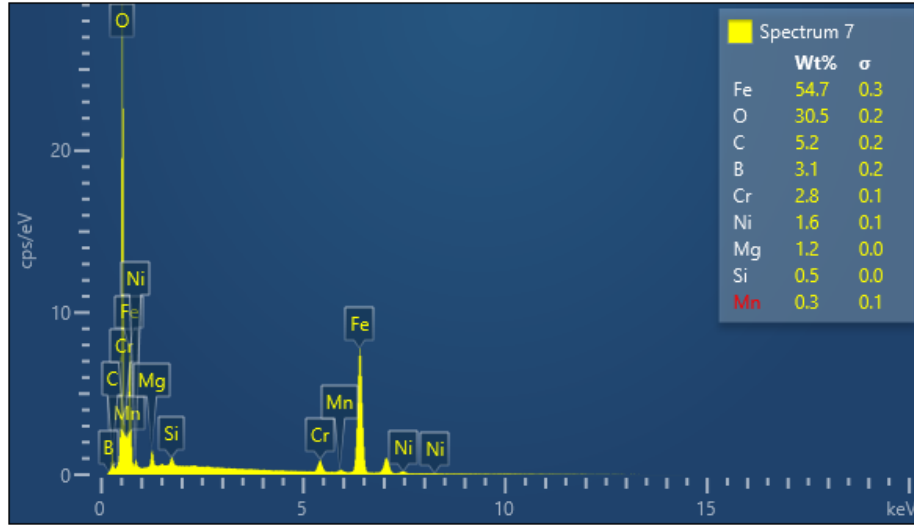
Figure 0-10 Composition of olivine calcinated in point 7 SEM figure 2.8

The figures 2.9 and 2.10 show the highest Fe content, coinciding with a similar surface apparency between them and different of points 5 and 8. The composition reveals an Fe increase from 5.7% as indicated in figure 2.7% to 54.7% in figure 2.10.
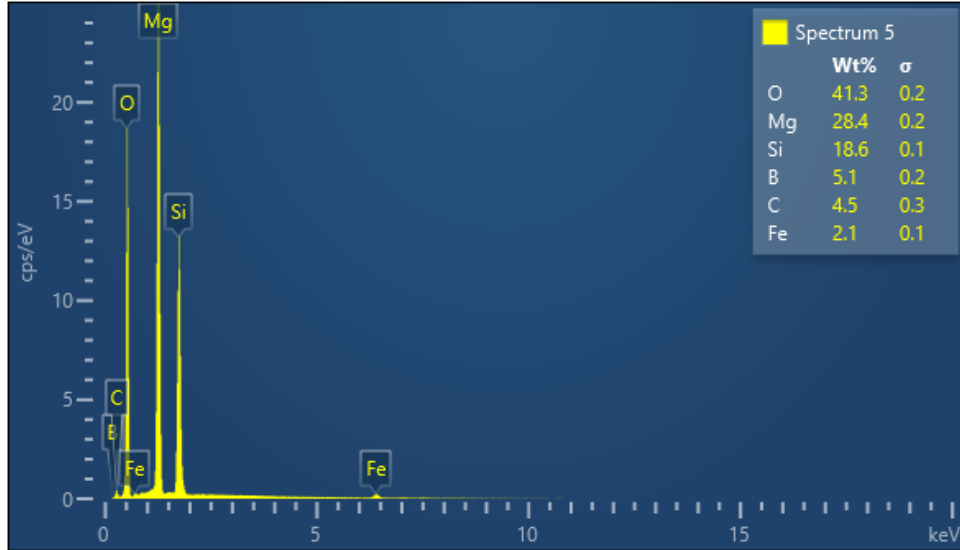
Figure 0-11 Composition of olivine calcinated in point 5 SEM figure 2.8
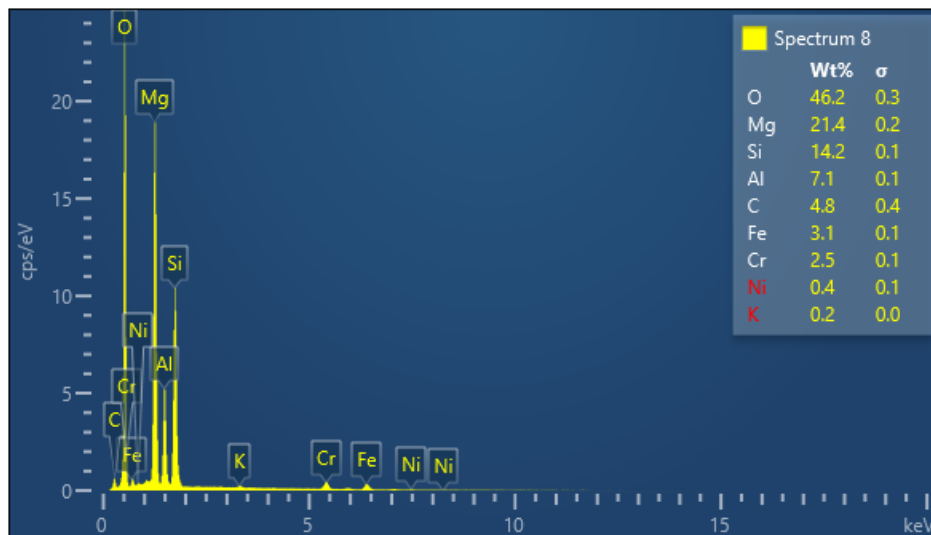
Figure 0-12 Composition of olivine calcinated in point 8 SEM figure 2.8

The Figures 2.11 and 2.12 reveal a low Fe content. The same phenomena is reported by (Devi, Craje, et al., 2005), where different calcination times were used and the presence of zones with a low Fe content is detected regardless of the calcination time. In this same work, the author shows how the atomic concentration on the surface of the olivine reaches a constant value after 5h of calcination. With this information, the temperature, time, and gas flow were selected to perform the respective calcination process in this experimental work.

2.7.2 Olivine reduction

The next step in the olivine treatment is the reduction of the Fe formed on the surface of the catalyst, in the form of Fe^{+3}, due to the oxidation caused by the oxygen present in the air, forming the respective ferric oxide, Fe_2O_3. The goal of the reduction is to convert the Fe^{+3} in Fe^0 or Fe metallic, using hydrogen as reducing agent. The work done by (Rauch et al., n.d.) takes different types of olivine and different calcination temperatures, showing the peaks of the H_2 consumption in the respective TPR, those peaks are between 650 °C and 710 °C, with a maximum temperature of 950 °C where the H_2 consumption is null. The temperature selected in this work was 700 °C for all the reduction processes. To keep constant the ratio of the H_2 used in the reduction, considering the time and the flow, keeping constant the temperature, it is defined the next parameter named HCR:

$$HCR = \frac{H_2 \, flow\left[\frac{Nl}{min}\right] * time[h]}{m_{cat}[kg]} = 6 \, \frac{Nl * h}{min * kg} \qquad 2$$

The value of 6 was kept constant under different catalyst charges, reduction time or hydrogen flows.

Figure 2.13 depicts macroscopically the changes undergone by olivine under different thermochemical treatments. In this case, untreated olivine exhibits a green color, although another olivine may appear brown. Calcined olivine displays a reddish color, typical of iron oxide Fe_2O_3, while the sample on the right illustrates reduced olivine, exhibiting a gray color characteristic of metallic iron.

Figure 0-13 Physical appearance of olivine

2.7.3 Pyrolysis experimental procedure

Once the weight of the empty condensers and biochar collector has been recorded, the amount of biomass to be processed (200 grams - 1000 grams) is deposited into the hopper. The hopper is then closed, and an airflow (5 Nl/min - 10 Nl/min) is initiated. The outlet valves are closed, increasing the pressure in the system to 10 psig. At this point, the system's integrity is checked for leaks in the reactor, condensers, and flow lines. Once the system's tightness is verified, the airflow is allowed to escape, and the pressure is regulated to 1 psig by adjusting the vacuum pressure in the respective gas exhaust line. The reactor is then heated while maintaining a constant airflow. Air is used to promote the combustion of any residues in the system and heat up all the components

reactor downstream. Once the system reaches the operating temperature, in this case, 625°C, the airflow is stopped and replaced with a constant flow of nitrogen, fixed at 2 Nl/min, and maintained for approximately 10 minutes until both the temperature and pressure have stabilized. The screw feeder is then turned on, transferring the biomass from the hopper into the reactor at a predetermined feeding rate. Upon biomass entry into the reactor, considered as time zero, a slight pressure increase is observed, and the nitrogen flow is suspended. The vacuum pressure in the exhaust line is adjusted to maintain a system pressure of 1 psig, initiating the extraction of the biochar generated at the bottom of the reactor. The reactor's agitator is kept rotating at 2 rpm, ensuring that all generated biochar is directed to the extraction point. The system operates without a carrier gas. Fifteen minutes after the pyrolysis reaction has started, the first gas sample is taken, and this process is repeated every 15 minutes or 30 minutes, depending on the amount of biomass being treated. Once the biomass is fully processed, the feeding is stopped, and a constant flow of nitrogen at 2 Nl/min is initiated. The biochar collector continues to operate, as does the reactor's agitator. When the system reaches 50°C, the nitrogen flow and biochar extraction are halted. The condensers are disconnected, and the biochar collector as well, the final weight is recorded for the respective calculations.

2.7.4 Pyrolysis thermal-catalytic-cracking-reforming procedure

This procedure incorporates some of the basic stages described for pyrolysis and calcination processes. Certain modifications regarding the timing of initiating the respective processes and valve adjustments enable the simultaneous heating of the pyrolysis reactor alongside the tubular reactor containing olivine. During the reduction of olivine, the heating of the pyrolysis reactor is carried out simultaneously using air. Upon completion of the olivine reduction, the airflow to the pyrolysis reactor is halted and replaced with nitrogen, which is directed towards the tubular reactor to continue heating it up to 950 °C. Once the temperature in the tubular reactor is reached, the biomass feeding into the pyrolysis reactor commences, and the same procedure outlined previously in the pyrolysis section is followed.

In the case of reforming with steam, a predetermined water flow is injected into the reactor. The vessel containing the water is always pressurized between 20 psig – 30 psig to overcome the

pressure drop due to the water flow trough the piping. The steam generated is injected at the bottom of the reactor allowing a previous expansion to equalize the pressure inside the reactor.

Chapter 3

3 Pyrolysis

3.1 Operating conditions

The respective operation parameters, temperature, pressure, and feed rate are summarized in Table 3.1.

Table 3-1 Conditions for pyrolysis experiments

	Feed rate (g/min)	Temperature (°C)	Pressure (psig)
PR01	2.78		
PR02	3.67		
PR03	5.00		
PR04	5.17		
PR05	6.67	625	1.0
PR06	7.41		
PR07	8.33		
PR08	9.60		
PR09	11.11		

3.2 Pyrolysis yields

The determination of the Yields is calculated as follows:

➢ **Biochar**: total weight of the biochar collected in the respective vessel. The calculation is:

$$Y_C = \frac{m_f^{Collector} - m_i^{Collector}}{Biomass} \qquad 3$$

Where:

$Y_C = Char\ Yield\ (Fraction)$

$m_f^{Collector} = Biochar\ collector\ final\ weigth\ (g)$

$m_i^{Collector} = Biochar\ collector\ initial\ weigth\ (g)$

$Biomass = Total\ biomass\ fed\ (g)$

➤ **Bio-oil (Vapors)**: Total weight of the vapors condensed in the four condensers.

$$Y_V = \frac{\sum_{j=1}^{4}\left(m_f^j - m_i^j\right)}{Biomass} \qquad\qquad 4$$

Where:

$$Y_V = Vapors\ (Bio - Oil)\ Yield\ (Fraction)$$
$$m_f^j = Condenser\ j\ final\ weigth\ (g)$$
$$m_i^j = Condenser\ j\ initial\ weigth\ (g)$$

The condensation of vapors was carried out using three condensers in series, submerged in a bath of cold water, whose temperature was maintained between 0°C and 5°C. A fourth condenser was used as a physical filter, its interior packed with cotton fiber. This last filter has a dual purpose in the process: firstly, as a final filter to retain VOC, and secondly, to regulate and maintain constant pressure in the system (1 psig). Below are the specifications of the implemented condensation train.

Table 3-2 Condensing train specifications

Condensing train	
Material	Stainless steel 316
Type	Condensing/Collecting descending layer
Heat transfer area (Total 3 units)	1370 cm^2
Collecting volume (Total 3 units)	1324 cm^3

It is imperative to consider the following with respect to the substance collected in the condensers. In the case of pyrolysis, the vapors, i.e., the gas-phase substances generated during pyrolysis and undergoing phase transition at a constant pressure of 1 psig at an approximate temperature of 5°C, are referred to as bio-oil. In the case of thermal cracking and catalytic cracking, the substances condensing under the conditions are termed tar or condensates. In certain instances, elucidation will be provided regarding the substances retained within the cotton filters, constituting a portion of the tar; however, owing to their vapor pressure properties and mass transfer to the gas phase, they may appear to persist as gases but are, in fact, classified as VOC, particularly aromatic compounds and/or PAH.

➢ **Gases**: Difference between the total biomass, Biochar and Vapors.

$$Y_G = 1 - Y_C - Y_V \qquad\qquad 5$$

Where:
$$Y_G = Gases\ Yield\ (Fraction)$$

The respective experimental yields obtained under the operational conditions listed in Table 3.1, are summarized in Table 3.3. These yields are based on the total biomass fed into the reactor. Considering this, the respective mass balances will primarily be calculated with reference to biomass-AR. The terms biomass and biomass-AR refer to the same material.

Table 3-3 Pyrolysis experimental yields

	Feed rate (g/min)	Biochar	Vapors	Gas
PR01	2.78	19.4%	32.3%	48.3%
PR02	3.67	18.2%	32.9%	48.9%
PR03	5.00	18.0%	32.0%	50.0%
PR04	5.17	18.4%	33.1%	48.5%
PR05	6.67	18.0%	34.2%	47.8%
PR06	7.41	18.4%	32.0%	49.6%
PR07	8.33	18.7%	33.4%	47.9%
PR08	9.60	18.0%	32.5%	49.5%
PR09	11.11	16.6%	32.6%	50.8%
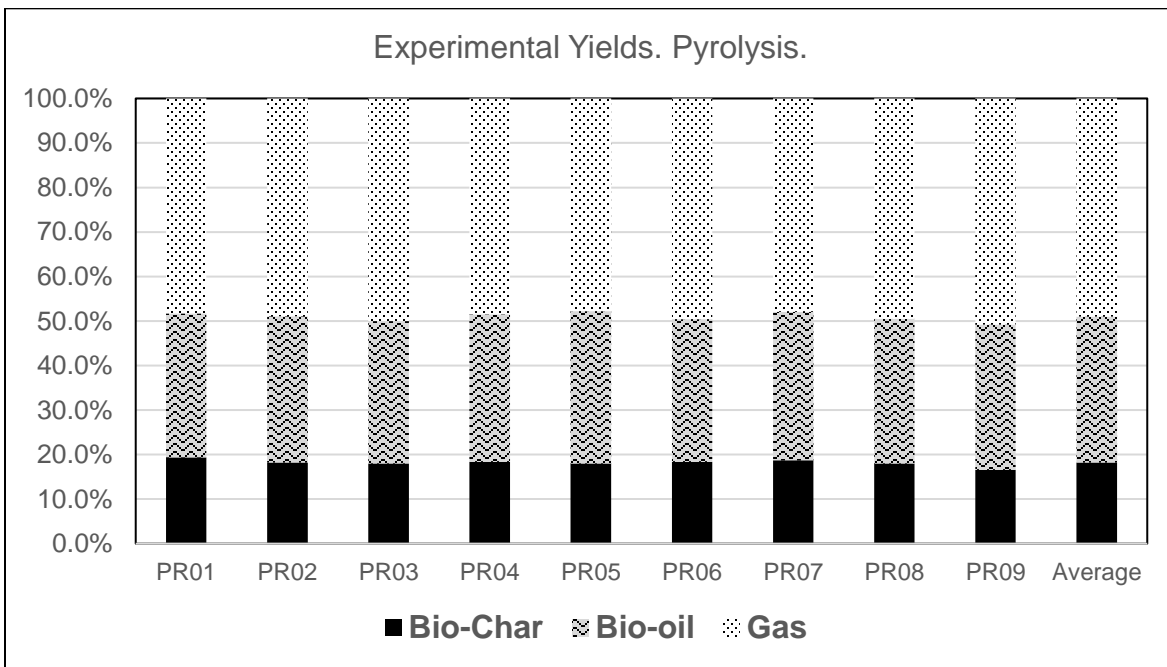
Figure 0-1 Pyrolysis yields

3.3 Yields analysis

Based on the literature and investigations conducted by various authors, such as (Di Blasi, 2009), the average yields of pyrolysis exhibit slight disparities compared to those obtained herein. The predominant consensus among them reports yields for bio-oil or vapors falling within the range of 50% to 70% (Mullen et al., 2010). Nevertheless, it is noteworthy that the yields of individual fractions arising from the pyrolysis of lignocellulosic materials are contingent upon factors including reactor type, particle size, residence time, heating rate, and notably, temperature, as elucidated by (Abou Rjeily, Cazier, et al., 2023).

24

Considering the conditions of the present study regarding temperature and particle size (2 mm – 4 mm), the work conducted by (L. Wang et al., 2022), exhibits significant similarity to the results obtained here, where the particle size and temperature chance the respective yields, being the values very close to the yields found in this work. Considering the various studies and the reproducibility of the experiments, as tabulated in Table 3.3, the arithmetic mean will be taken as the value to be used in the base case of pyrolysis.

3.4 Compositions

The composition for each one of the fractions is described next.

3.4.1 Biochar composition

The experimental composition of the biochar for each one of the experiments is tabulated in Table 3.4. This composition was determined by the "Elemental Analyzer Flash EA 1112" series used in the biomass elemental analysis.

Table 3-4 Experimental biochar composition

	PR01	PR02	PR03	PR04	PR05	PR06	PR07	PR08	PR09
C	78.52%	77.00%	77.02%	78.60%	77.34%	76.87%	76.60%	77.00%	76.20%
H	2.86%	2.90%	2.61%	2.99%	2.65%	3.01%	2.96%	3.00%	2.51%
O	13.32%	14.44%	14.65%	12.81%	14.28%	14.52%	14.93%	14.28%	15.09%
Ash	5.30%	5.66%	5.72%	5.60%	5.73%	5.60%	5.51%	5.72%	6.20%

The figures 3.2 and 3.3 show the variation of the Biochar composition as a function of the feed rate into the pyrolysis reactor.
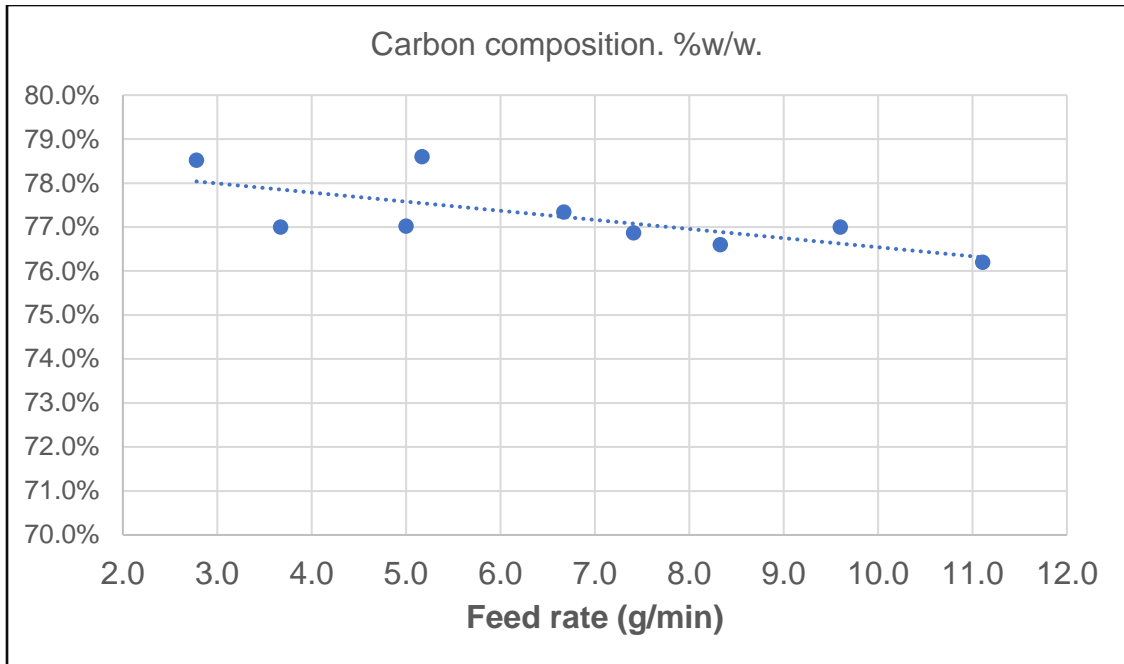
Figure 0-2 Carbon composition of biochar
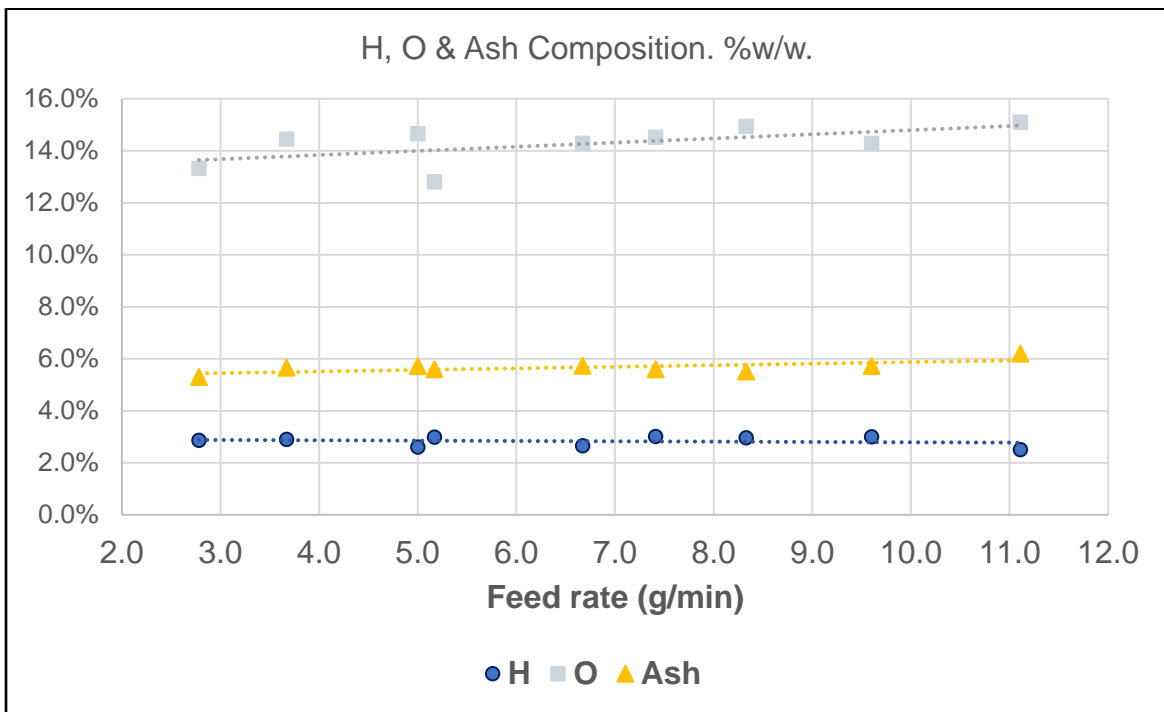
Figure 0-3 Hydrogen, oxygen, and ash composition of biochar

The corresponding elemental amounts for C, H and O present in the Biochar are calculated as follows:

$$C_C = Biomass * Y_C * x_C^C \qquad\qquad 6$$

$$H_C = Biomass * Y_C * x_C^H \qquad\qquad 7$$

$$O_C = Biomass * Y_C * x_C^O \qquad\qquad 8$$

Where:

$C_C = Carbon\ mass\ present\ in\ Biochar\ (g)$

$H_C = Hydrogen\ mass\ present\ in\ Biochar\ (g)$

$O_C = Oxygen\ mass\ present\ in\ Biochar\ (g)$

$x_C^C = Carbon\ mass\ fraction\ (from\ Elemental\ analysis)\ in\ Biochar.$

$x_C^H = Hydrogen\ mass\ fraction\ (from\ Elemental\ analysis)\ in\ Biochar.$

$x_C^O = Oxygen\ mass\ fraction\ (from\ Elemental\ analysis)\ in\ Biochar.$

3.4.2 Gas composition

The gas composition is determined using the analytical technique Micro-GC. The average molar composition of the gas is summarized in table 3.6. It is important to note that the average composition reported in table 3.6 represents the arithmetic average for each of the experiments from the samples taken at different times after the beginning of the respective experiment. The first sample was taken 15 minutes after the biomass feeding started to the pyrolysis reactor, followed by samples taken every 15 minutes thereafter. This procedure was applied for experiments PR03, PR04, PR05, PR06, PR07, PR08, and PR09. In the case of experiments PR01 and PR02, only one sample was taken at 20 minutes after starting the feeding.

The fraction named C_2-C_4 correspond to the gases: C_2H_4, C_2H_6, C_3H_6, C_3H_8, C_4H_{10}. These gases are named secondary gases, and the gases H_2, CH_4, CO and CO_2 are the main gases.

The relative percentage of each one of the secondary gases is taken from the detailed gas analysis for each one of the experiments and summarized in the table 3-5.

Table 3-5 C2-C4 percentages in pyrolysis gases

Relative composition for the C_2-C_4 fraction.	
C_2H_4	35.36%
C_2H_6	21.68%
C_3H_6	15.54%
C_3H_8	20.40%
C_4H_{10}	7.02%

Table 3-6 Gas composition as a function of feed rate

	Feed rate. (g/min)	H_2	CH_4	CO	CO_2	C_2-C_4
PR01	2.78	12.05%	14.87%	45.29%	19.27%	8.52%
PR02	3.67	11.89%	14.20%	44.55%	20.63%	8.73%
PR03	5.00	10.70%	14.25%	45.50%	20.88%	8.67%
PR04	5.17	10.68%	14.29%	45.53%	21.54%	7.96%
PR05	6.67	10.46%	14.07%	46.25%	22.28%	6.94%
PR06	7.41	10.45%	13.22%	47.45%	21.78%	7.10%
PR07	8.33	10.76%	13.79%	46.22%	21.74%	7.48%
PR08	9.60	10.37%	13.33%	46.79%	21.85%	7.66%
PR09	11.11	9.99%	13.33%	43.96%	24.57%	8.15%

The graphical representation of the main gases and the grouped secondary gases are shown in Figures 3.4 and 3.5.
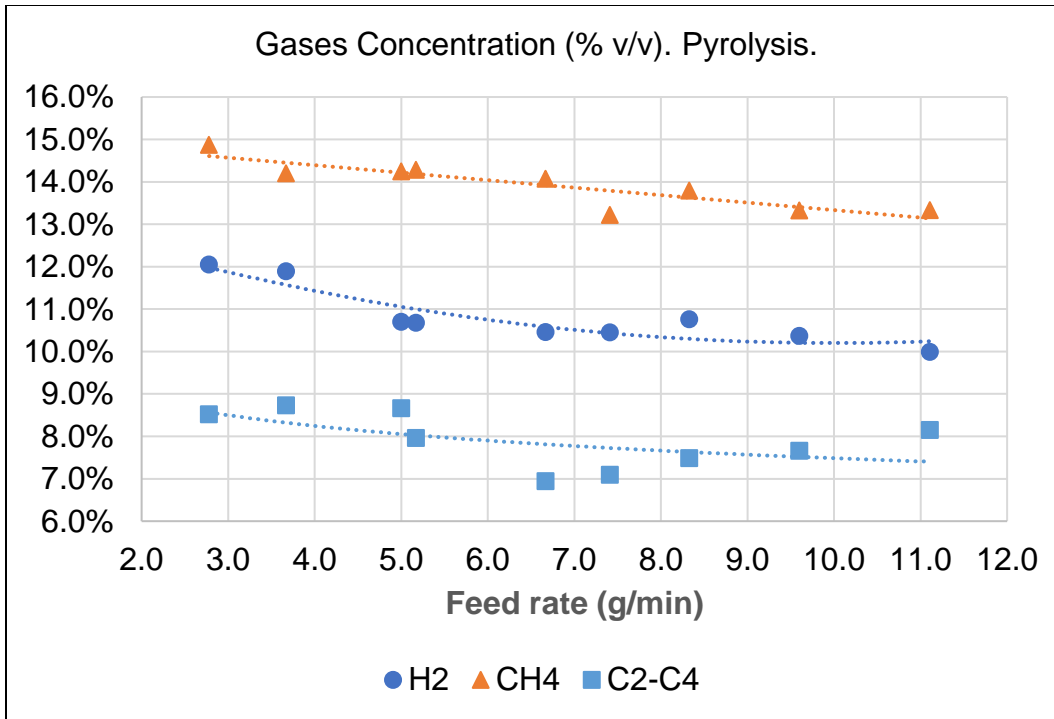
Figure 0-4 H_2, CH_4, and C_2-C_4 concentration as a function of feed rate
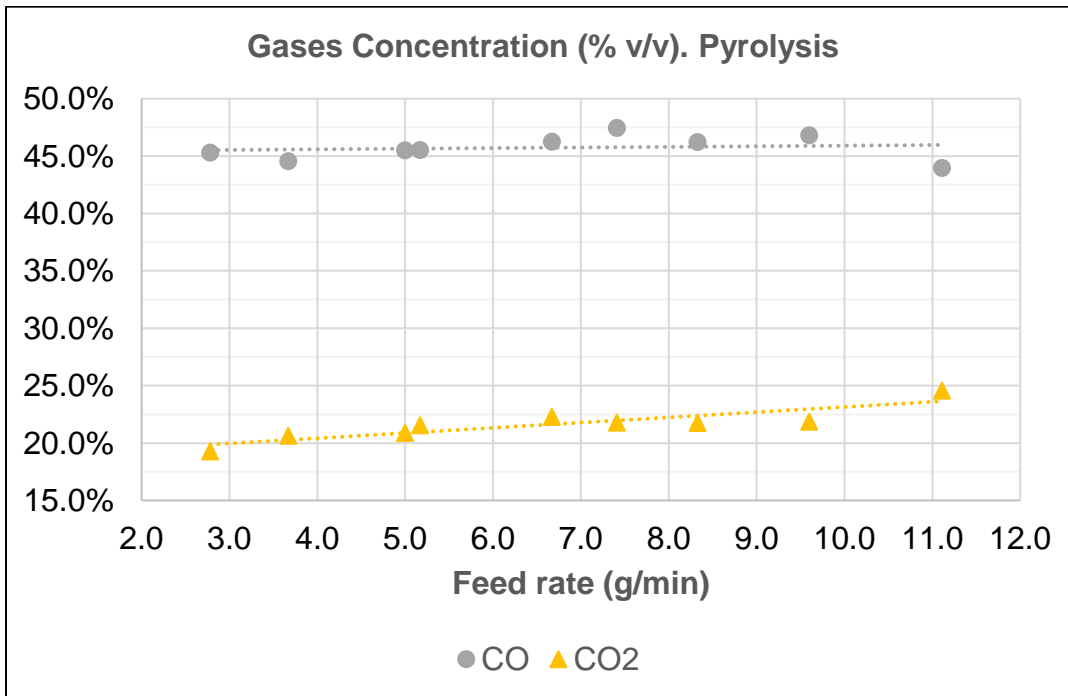
Figure 0-5 CO and CO_2 concentration as a function of feed rate

Regarding about the calculation of the C, H and O content in the Gas fraction, the procedure is described next.

29

➢ **Calculation of Average Molecular Weight for the Gas**.

$$\overline{MW_G} = \sum_{k=1}^{9} y_G^k * MW^k \qquad\qquad 9$$

Where:

$\overline{MW_G} = Gas\ Average\ molecular\ weight\ \left(\frac{g}{mole}\right)$

$y_G^k = Volumetric\ Fraction\ of\ specie\ k\ in\ gas$

$MW^k = Molecular\ Weight\ specie\ k.$

The substances present in the gas and their respective k index and molecular weight are listed below:

Table 3-7 Gases coefficients

Specie	k	MW (g/mol)	ξ_C	ξ_H	ξ_O
H_2	1	2	0	2	0
CH_4	2	16	1	4	0
CO	3	28	1	0	1
CO_2	4	44	1	0	2
C_2H_4	5	28	2	4	0
C_2H_6	6	30	2	6	0
C_3H_6	7	42	3	6	0
C_3H_8	8	44	3	8	0
C_4H_{10}	9	58	4	10	0

➢ **Calculation of the elemental amount of C, H, and O present in the gas**.

$$C_G = \sum_{k=1}^{9} \left(\frac{Biomass * Y_G}{\overline{MW_G}}\right) * y_G^k * \xi_C^k * 12 \qquad\qquad 10$$

$$H_G = \sum_{k=1}^{9} \left(\frac{Biomass * Y_G}{\overline{MW_G}}\right) * y_G^k * \xi_H^k * 1 \qquad\qquad 11$$

$$O_G = \sum_{k=1}^{9} \left(\frac{Biomass * Y_G}{\overline{MW_G}}\right) * y_G^k * \xi_O^k * 16 \qquad\qquad 12$$

Where:

$C_G = Carbon\ mass\ present\ in\ Gas\ (g)$

$H_G = Hydrogen\ mass\ present\ in\ Gas\ (g)$

$O_G = Oxygen\ mass\ present\ in\ Gas\ (g)$

$\xi_C^k = Number\ of\ Carbon\ atoms\ in\ specie\ k.$

$\xi_H^k = Number\ of\ Hydrogen\ atoms\ in\ specie\ k.$

$\xi_O^k = Number\ of\ Oxygen\ atoms\ in\ specie\ k.$

3.4.3 Bio-oil (Vapors) composition

The condensable fraction of the vapor phase is known as bio-oil if it is condensed and collected, or vapors (in this work) when it remains in its vapor phase. The composition of the vapors is a mixture of numerous different substances, as studied and reported by several authors.

The work of (Azeez et al., 2010) reported 80 species present in the spruce bio-oil, another researcher reported 22 species present (Mullen et al., 2010). Regarding the modeling of bio-oil conversion and/or cracking/reforming to gas, other authors report the analysis according to elemental analysis (CHO content). This approach enables the representation of bio-oil as a surrogate, as reported by (Bridgwater, 2012).

The application of models varies according to the study's objectives. In this case, for mass balance purposes, utilizing elemental analysis and the respective surrogate generated is ideal. Here, a combination of both models will be employed for bio-oil analysis. The surrogate will be utilized for mass balance calculations, while the compositional model will be employed to derive some thermodynamic and transport properties.

According to the work done by (Fu et al., 2014), the main species identified could be reduced to 20 known substances, so the thermodynamic, and transport properties are easily computed using, for example a chemical process simulation program, that in this case will be Aspen Plus V12.0.

The final water content in the bio-oil modifies the surrogate composition and the detailed one, so according to the water content, and the atomic balance linked with the respective yields, representation of the bio-oil as a continuous thermodynamic substance is expressed as: $\boldsymbol{CH_y O_z}$

The water content has been investigated by several authors, among the studies, the works done by (Di Blasi, 2009), and (Fu et al., 2014), have indicated that the pyrolytic water, or the water

generated due to the pyrolysis of the biomass, corresponds to an average value of 10% of the DAF of the original biomass.

The total amount of water present in Vapors is calculated according to:

$$H_2O^M = Biomass * M^{AR} \tag{13}$$

$$H_2O^{PR} = Biomass * (1 - Ash - M^{AR}) * 0.1 \tag{14}$$

$$H_2O_V = H_2O^M + H_2O^{PR} \tag{15}$$

Where:

$H_2O^M = Water\ as\ moisture\ in\ the\ original\ Biomass\_AR\ (g)$

$H_2O^{PR} = Water\ generated\ by\ pryolysis\ (g)\ (10\%\ of\ the\ Biomass\_DAF)$

$M^{AR} = Moisture\ content\ in\ Biomass\_AR\ (fraction)$

$Ash = Ash\ content\ in\ Biomass\_AR$

$H_2O_V = Total\ water\ in\ vapors\ stream\ (g)$

With the respective water content calculated, the gas composition, and biochar composition, the atomic (C, H, O) mass balance is calculated as follows:

$$C_V = Biomass * x_C^{B\_AR} - C_C - C_G \tag{16}$$

$$H_V = Biomass * x_H^{B\_AR} - H_C - H_G - H_2O^{PR} * \left(^2/_{18}\right) \tag{17}$$

$$O_V = Biomass * x_O^{B\_AR} - O_C - O_G - H_2O^{PR} * \left(^{16}/_{18}\right) \tag{18}$$

Where:

$C_V = Carbon\ mass\ present\ in\ Vapors\ (g)$

$H_V = Hydrogen\ mass\ present\ in\ Vapors\ (g)$

$O_V = Oxygen\ mass\ present\ in\ Vapors\ (g)$

$x_C^{B\_AR} = Carbon\ mass\ fraction\ (from\ Elemental\ analysis)\ in\ Biomass\_AR$

$x_H^{B\_AR} = Hydrogen\ mass\ fraction\ (from\ Elemental\ analysis)\ in\ Biomass\_AR$

$x_O^{B\_AR} = Oxygen\ mass\ fraction\ (from\ Elemental\ analysis)\ in\ Biomass\_AR$

Taking these values and the respective material balance for each one of the Pyrolysis experiments, the coefficients for the chemical model CH_yO_z, are calculated as follows:

$$y = \frac{H_V * 12}{C_V} \qquad\qquad 19$$

$$z = \frac{O_V * 12}{C_V * 16} \qquad\qquad 20$$

The values calculated for each one of the pyrolysis experiments are summarized in table 3.9. The elemental balance results for each experiment show consistent values, indicating consistency in the analyses of biochar and gases. Although slightly different from literature values, especially in hydrogen content which is slightly higher, the obtained values will be used for calculations.

Table 3-8 Calculated coefficients for bio-oil (vapors) surrogate (CH_yO_z)

	C	H	O
PR01	1	2.85	0.81
PR02	1	2.57	0.65
PR03	1	2.80	0.62
PR04	1	2.75	0.66
PR05	1	2.67	0.55
PR06	1	2.87	0.51
PR07	1	2.72	0.56
PR08	1	2.77	0.52
PR09	1	2.62	0.41

Some of the reported Surrogates by authors are listed below.

Table 0-9 Reported bio-oil surrogate formula

Author	Reported bio-oil formula. CH_yO_z.
(Bridgwater, 2012)	$CH_{1.33}O_{0.43}$
(Radlein et al., 1991)	$CH_{1.47}O_{0.67}$
(D. Wang et al., 1997)	$CH_{1.33}O_{0.53}$
	$CH_{1.47}O_{0.60}$
	$CH_{1.52}O_{0.76}$

The alternative model to represent the bio-oil as a complex mixture of tenths to hundreds of substances require an extensive and detailed analysis of the bio-oil. The work done by (Choi et al.,

2014) identified 52 substances, (Debiagi et al., 2016) represent the bio-oil as a mixture of 26 components. Some of these common substances for all the reported by the authors are listed in the table below:

Table 0-10 Selected major organic compounds in bio-oil.

Name	C	H	O
Formaldehyde	1	2	1
Formic acid	1	2	2
Methanol	1	4	1
Glyoxal	2	2	2
Acetaldehyde	2	4	1
Acetic Acid	2	4	2
Ethanol	2	6	1
Acrolein	3	4	1
Propionaldehyde	3	6	1
Propanoic acid	3	6	2
2-Furaldehyde	5	4	2
Xylofuranose	5	8	4
Phenol	6	6	1
5-Hydroxymethyl furfural	6	6	3
Levoglucosan	6	10	5
Cresol	7	8	1
Vanillin	8	8	3
Linalyl propionate	13	22	2
Methyl Linoleate	19	34	2
Heavy molecular lignin	24	28	4

The detailed description of bio-oil (vapors) is beneficial for explaining the maximum theoretical yields of each substance when cracked or reformed using steam as a reforming agent. Additionally, it provides valuable thermophysical information. An example of this approach is the done by (Palla et al., 2015), where the authors model the bio-oil as a mixture of 11 very known substances to get all the thermodynamic and transport properties data necessary to a detailed numerical modelling. Using HPLC analysis, the aqueous fraction of the collected bio-oil was analyzed to verify the presence of some of the substances mentioned in the table. It is important to clarify that the analysis is solely qualitative and not quantitative. Figure 3.6 shows the results of HPLC analysis.

<Chromatogram>

mV

Detector A Channel 1
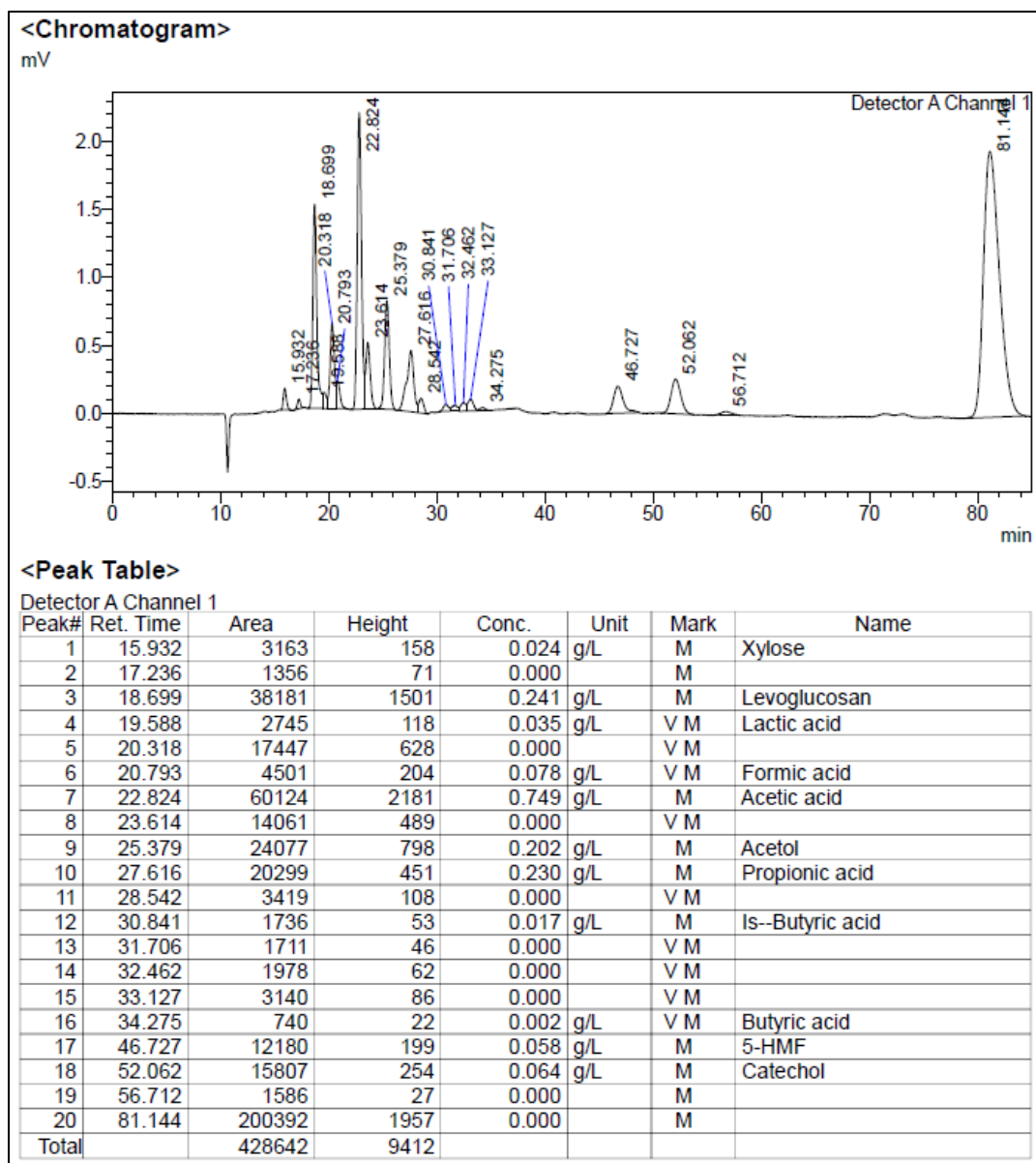
Figure 0-6 HPLC for aqueous fraction bio-oil pyrolysis

<Peak Table>

Detector A Channel 1

Peak#	Ret. Time	Area	Height	Conc.	Unit	Mark	Name
1	15.932	3163	158	0.024	g/L	M	Xylose
2	17.236	1356	71	0.000		M	
3	18.699	38181	1501	0.241	g/L	M	Levoglucosan
4	19.588	2745	118	0.035	g/L	V M	Lactic acid
5	20.318	17447	628	0.000		V M	
6	20.793	4501	204	0.078	g/L	V M	Formic acid
7	22.824	60124	2181	0.749	g/L	M	Acetic acid
8	23.614	14061	489	0.000		V M	
9	25.379	24077	798	0.202	g/L	M	Acetol
10	27.616	20299	451	0.230	g/L	M	Propionic acid
11	28.542	3419	108	0.000		V M	
12	30.841	1736	53	0.017	g/L	M	Is--Butyric acid
13	31.706	1711	46	0.000		V M	
14	32.462	1978	62	0.000		V M	
15	33.127	3140	86	0.000		V M	
16	34.275	740	22	0.002	g/L	V M	Butyric acid
17	46.727	12180	199	0.058	g/L	M	5-HMF
18	52.062	15807	254	0.064	g/L	M	Catechol
19	56.712	1586	27	0.000		M	
20	81.144	200392	1957	0.000		M	
Total		428642	9412				

Some of the components named in table 3.11 are not identified, in the respective chromatogram, but as was mentioned before, this is just the aqueous fraction of the bio-oil.

3.4.4 PAH composition

One of the objectives of the current study is to evaluate the capability of olivine to convert PAH into H_2 and CO. To assess this capacity without installing the compound capture system according to the EU/IEA/US-DOE protocol, a physical filtering system located downstream the condenser

and submerged in the same water bath was installed. The filtering medium consists of 100% cotton fibers compacted to achieve an approximate density of 0.5 g/cm^3. The approximate volume of the filter is 300 cm^3. Upon completion of the experimental phase, the cotton filter is removed, and the trapped components are extracted from the filter. Extraction is carried out using Isopropanol as a solvent employing the Soxhlet method for 24 hours. Subsequently, a sample of the extract is taken and analyzed using GC/MS. The results for the filters used in pyrolysis are presented below in figure 3.7.

The database used to compare the results of the Chromatogram shown in Figure 3.8 correspond to the NIST database. The components with the highest match factor are listed in table 3.12.
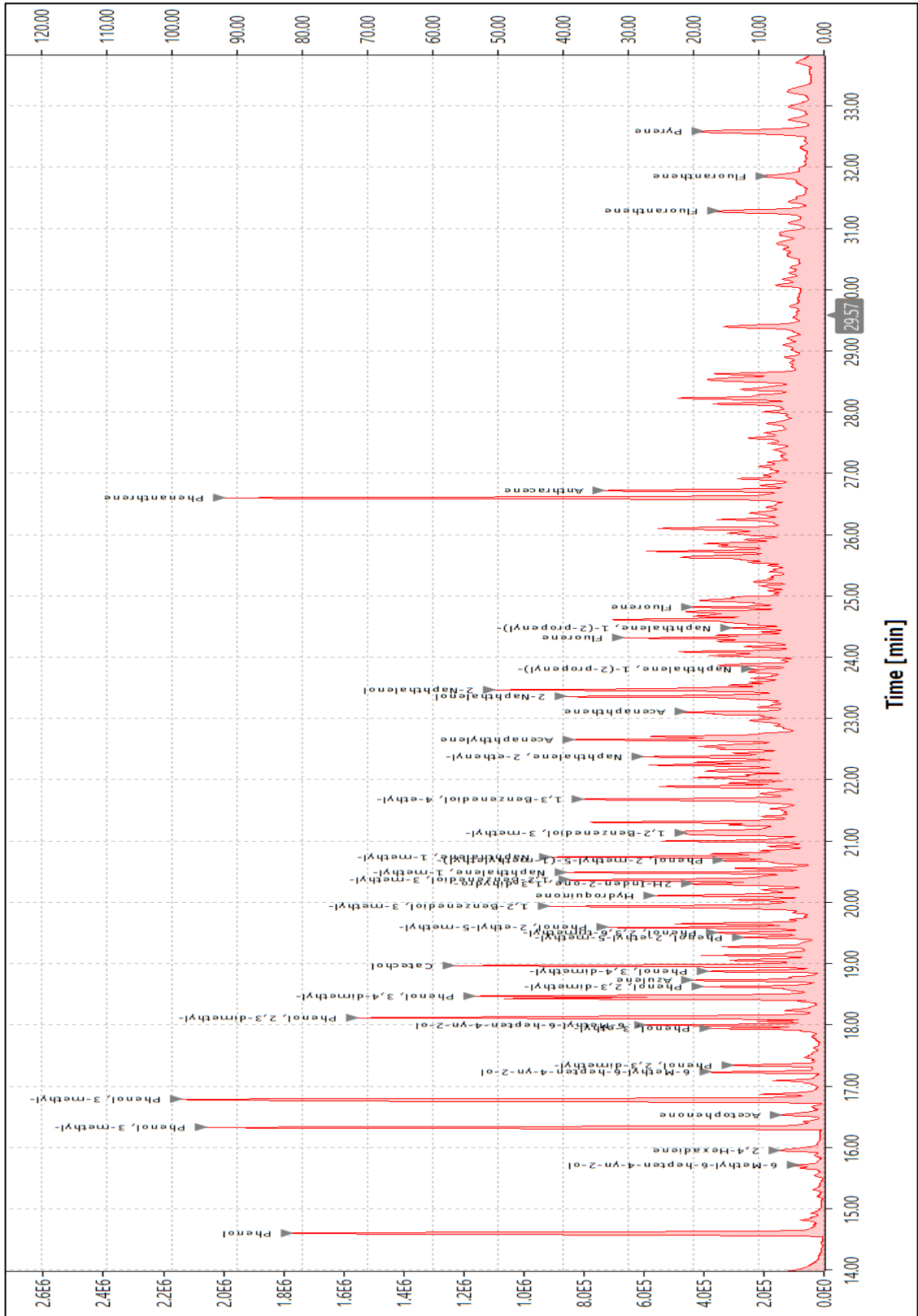
Figure 0-7 GC/MS result for pyrolysis tar

Table 3-11 PAH identified in pyrolysis baseline case

ID	Substance
1	1,2-Benzenediol, 3-methyl-
2	1,3-Benzenediol, 4-ethyl-
3	2,4-Hexadiene
4	2H-Inden-2-one, 1,3-dihydro-
5	2-Naphthalenol
6	6-Methyl-6-hepten-4-yn-2-ol
7	Acenaphthene
8	Acenaphthylene
9	Acetophenone
10	Anthracene
11	Azulene
12	Benz[j]aceanthrylene,
13	Benzo[a]pyrene
14	Catechol
15	Fluoranthene
16	Fluorene
17	Hydroquinone
18	Naphthalene, 1-(2-propenyl)-
19	Naphthalene, 1-methyl-
20	Naphthalene, 2-ethenyl-
21	Phenanthrene
22	Phenol
23	Phenol, 2,3,6-trimethyl-
24	Phenol, 2,3-dimethyl-
25	Phenol, 2-ethyl-5-methyl-
26	Phenol, 2-methyl-5-(1-methylethyl)-
27	Phenol, 3,4-dimethyl-
28	Phenol, 3-ethyl-
29	Pyrene

These results are going to be used as pyrolysis baseline case to compare the capacity of the olivine in the destruction of those substances into H_2 and CO and smaller molecules.

The physical appearance of the filter after the experimental procedure is going to be an indicator of the capacity of transforming the PAH into useful gases.

Figure 3.8 show the physical appearance of the filter after the experiment.

Figure 0-8 PAH trapped in cotton filter Pyrolysis experiments

Regarding about the total PAH (Most of the authors report the aromatic components as TAR), (Brage et al., 1996) reports at 700 ºC a total of 42 g/kg, meanwhile, (Vassilatos et al., 1992), reported almost the same amount of total TAR at the same temperature (aromatics and PAH), this author show a very useful graph of how the total tar is a function of the thermal cracking temperature. Using this graph and extrapolating the function, the quantity of PAH generated at 625 ºC takes a value close to 45 g/kg. It is important to clarify that in this work the quantitative determination for the PAH is not determined. The value of 45 g/kg correspond to approximately the 4.5 % of the Biomass fed to the reactor and this value is not included in the mass balance.

3.5 Pyrolysis baseline case
The pyrolysis baseline case is established from experimental data. The average data concerning yields and composition of each fraction (biochar-vapors-gas) serves as the reference point for evaluating the effectiveness of thermal cracking, catalytic cracking, and catalytic steaming.
The values for this pyrolysis baseline are indicated in the following tables:

Table 3-12 PRBC yields

Average Yields (% mass)	
Biochar	18.2%
Vapors	32.8%
Gases	49.0%

Table 3-13 PRBC biochar composition

Biochar Composition (% mass)	
C	77.2%
H	2.8%
O	14.3%
Ash	5.7%

Table 3-14 PRBC gas composition

Gas	Pyrolysis		Gas	Pyrolysis
H_2	10.82%		H_2	10.82%
CH_4	13.93%		CH_4	13.93%
CO	45.73%		CO	45.73%
CO_2	21.62%		CO_2	21.62%
C_2H_4	2.80%		C_2-C_4	7.91%
C_2H_6	1.72%			
C_3H_6	1.23%			
C_3H_8	1.61%			
C_4H_{10}	0.56%			

The respective formula for the surrogate regarding the Bio-Oil (Vapors) is given by:

$$CH_{2.74}O_{0.59}$$
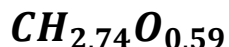
One of the main objectives of this work is to increase the amount of hydrogen in the gas while converting heavy hydrocarbons present in the vapor phase, as well as the C2-C4 fraction, into H_2 and CO. To evaluate this, the net amount of hydrogen and other gases will be calculated in terms of mass. The respective values calculated for the pyrolysis baseline are tabulated below:

Table 3-15 PRBC net gas mass production

Specie	g/100 g biomass
H_2	0.384
CH_4	3.955
CO	22.722
CO_2	16.882
C_2-C_4	5.057

The mass composition of the Vapor fraction is calculated as:

Table 3-16 Net mass in vapor fraction

Substance	g/100 g biomass
Water	15.783
$CH_{2.27}O_{0.59}$	17.017

The approximate composition of the Vapors, considering the substances from table 3.10, and solving the model to minimize the error between the theorical mass fraction and the numerical solution, gives the composition listed in the table 3.15.

Table 3-17 PRBC theorical composition

Substance	%Mass
Levoglucosan	29.075
Linalyl propionate	24.499
Acetic Acid	19.557
Ethanol	11.006
Methanol	10.974
Acetaldehyde	1.096
Formaldehyde	1.063
Formic acid	1.013
Methyl Linoleate	0.509
Xylofuranose	0.274
Heavy molecular lignin	0.231
Propionaldehyde	0.231
2-Furaldehyde	0.138
Vanillin	0.111
Cresol	0.053
5-Hydroxymethyl furfural	0.042
Acrolein	0.040
Glyoxal	0.032
Propanoic acid	0.032
Phenol	0.026

The error in the model is summarized in the table below:

Table 3-18 Error in vapors composition

	% C	%H	%O
Mass Balance ($CH_{2.74}O_{0.59}$)	49.98	11.40	38.62
Numerical (Substances Table 3.17)	51.22	8.83	39.95
%Error	**2.49%**	**-22.55%**	**3.43%**

The first 10 substances in table 3.17 (Levoglucosan to Xylofuranose) sum the 99% of the total composition, so those substances will be used to get the respective thermodynamic and transport properties. It is very important to note that the composition of the bio-oil will be used only to model some of the thermophysical properties of the mixture going into the cracking reactor, but the mass balance will be done taking the surrogate model to have exact values in the mass balances. Taking in consideration the respective gas composition and the theorical vapor (bio-oil) water free composition, the mixture gas-vapor that will be treated in the cracking-reforming reactor, has the next mass composition taking 100 g of biomass as the baseline.

Table 3-19 PRBC composition model for gas & vapors. 100 g biomass

	Mass (g)	Gas	Molar Fraction
Gases	**49.000**	H_2	0.1082
		CH_4	0.1393
		CO	0.4573
		CO_2	0.2162
		C_2H_4	0.0280
		C_2H_6	0.0172
		C_3H_6	0.0123
		C_3H_8	0.0161
		C_4H_{10}	0.0056
	Mass (g)	**Substance**	**Mass Fraction**
Vapors/ Bio-Oil Water Free	**17.017**	Levoglucosan	0.2930
		Linalyl propionate	0.2473
		Acetic Acid	0.1974
		Ethanol	0.1111
		Methanol	0.1108
		Acetaldehyde	0.0111
		Formaldehyde	0.0107
		Formic acid	0.0102
		Methyl Linoleate	0.0051

		Xylofuranose	0.0028
Total Water	**Mass (g)**	**Substance**	**Mass Fraction**
	15.783	H_2O	1.000

4 Thermal cracking (TC)

4.1 Operating Conditions

The evaluation of thermal cracking for the upgrading of gases and vapors was conducted using a PFR reactor in series with the CSTR reactor employed for pyrolysis. Gases and vapors generated in the CSTR pyrolysis reactor were introduced into PFR, and then the cracked stream was cooled down to obtain the final tar. Samples of the syngas produced were taken periodically during the operation. The pyrolysis conditions (temperature, pressure) were maintained constant for all experiments.

Table 4-1 Thermal cracking conditions

PFR max volume (cm^3)	Temperature (K)	Pressure (psig)
595-1190	1223	1.0

4.2 Cases type I. Fixed volume

The first thermal cracking experiments were conducted, with a variable biomass feed rate into the pyrolysis unit and a constant thermal cracking reactor volume.

Table 4-2 Operational conditions for thermal cracking. Cases type I

	Biomass feed rate (g/min)	Pyrolysis gas-vapors flow @625 C 1psig (cm^3/s)	Pyrolysis gas-vapors flow @950 C 1psig (cm^3/s)	Volume PFR (cm^3)
TC01	5.00	165.2	225.0	
TC02	6.67	220.3	300.0	595
TC03	11.11	367.1	500.0	

The data to calculate the volumetric flow of the gases and vapors flowing to the cracking reactor, was obtained using the software Aspen Plus V12.0. Taking the composition indicated in the table 3.20, the next equation represents the specific volume of the pyrolysis gases-vapor mixture between 625 ºC and 950 ºC.

$$\vartheta_{VG} \left[cm^3/g \right] = 737.2 + 2.7 * T(°C) \qquad 21$$

The composition of the Cracked gas is shown next table:

Table 4-3 Syngas composition. Thermal cracking. Cases type I

	Syngas flow (g/min)	H$_2$	CH$_4$	CO	CO$_2$	C$_2$-C$_3$
TC01	3.330	28.3%	14.4%	39.0%	16.2%	2.1%
TC02	4.445	28.2%	13.5%	38.5%	16.7%	3.0%
TC03	7.156	26.0%	14.8%	39.2%	15.5%	4.5%

Using the correlation regarding the specific volume and the gases-vapors mass flow rate indicated in table 4.3, the respective residence time calculated at both temperatures, for each one of the experiments is tabulated next:

Table 4-4 Residence time for vapors-gases. Cases Type I

	Residence time pyrolysis vapors @625 C 1psig (s)	Residence time pyrolysis vapors @950 C 1psig (s)
TC01	4.425	3.249
TC02	3.315	2.434
TC03	2.059	1.512

The residence time is calculated according to the definition:

$$\tau(s) = \frac{V^{Reactor}[cm^3]}{\vartheta_{VG} \left[cm^3/g \right] * \dot{m}_{VG}[g/min] * \left[1\, min/60s \right]} \qquad 22$$

The final tar (condensable fraction) collected for each one of the experiments is shown in table 4.5. The Pyrolysis Baseline Case is tabulated as well to comparison.

Table 4-5 Final tar collected. Cases type I

	Pyrolysis	TC01	TC02	TC03
Final tar	32.8%	15.2%	15.1%	17.4%

The table 4.6. shows the comparison against the PRBC, regarding the net mass production for the main gases and the secondary gases grouped as C_2-C_3. In this case, the secondary gases are labeled in this way because the micro-GC analysis didn't identify the substance C_4 (n-butane).

Table 4-6 Comparison gas mass production. Cases type I

	g/100 g biomass			
	Pyrolysis	TC01	TC02	TC03
H₂	0.384	1.746	1.710	1.511
CH₄	3.955	7.113	6.564	6.869
CO	22.722	33.649	32.664	31.936
CO₂	16.882	21.939	22.305	19.862
C₂-C₃	5.057	2.154	3.428	4.222

4.3 Cases type II. Volume variable

The second type of experiments involved maintaining a constant biomass feed rate, as in the case of TC02, while varying the volume available for the reaction to observe its effect. The results are shown below:

Table 4-7 Syngas composition. Cases type II

	Feed rate (g/min)	Volume TC (cm³)	H₂	CH₄	CO	CO₂	C₂-C₃
TC02		595	28.2%	13.5%	38.5%	16.7%	3.0%
TC02A	6.67	866	28.5%	13.6%	38.3%	16.7%	3.0%
TC02B		1190	28.0%	13.4%	38.9%	16.6%	3.0%
TC02C		1190	28.9%	13.7%	38.1%	16.4%	2.9%

The global mass balance to the thermal cracking is tabulated below:

Table 4-8 Mass balance for TC experiments

	TC02	TC02-A	TC02-B	TC02-C	Average
Final Tar	15.10%	15.48%	15.23%	15.46%	**15.32%**

4.4 TAR and PAH analysis

The scope of this work is the upgrading of vapors and gases, so the quantitative analysis is focused on the gas fraction, meanwhile on the tar collected there is just a qualitative analysis to observe the change in the final tar collected. The next figure shows the aspect of the tar collected after the thermal cracking process. The figures 4.1 and 4.2 show the final tar (liquids) and filter with the PAH substances captured.
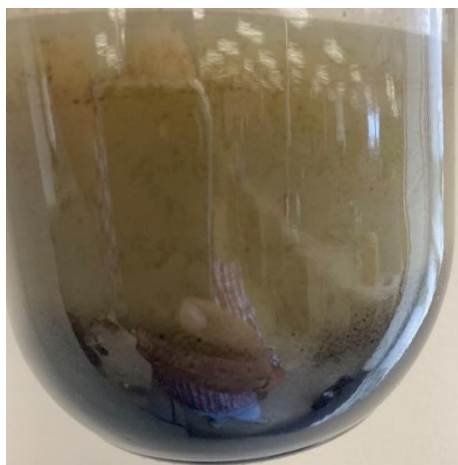
Figure 0-1 Final tar (Condensable) collected. TC

Figure 0-2 PAHs trapped in cotton filter. TC

The cotton filter and the collected final liquid reveal the positive effect of thermal cracking in converting part of the vapors into gases. This is evidenced not only by the decrease in the amount of collected liquids but also by the change in the physical appearance of the collected liquids, which no longer exhibit the original characteristics of bio-oil. The presence of high molecular weight substances is indicated by a cloudy appearance in the final condensates.

On the cotton filter, a decrease in retained substances is observed, which is corroborated by the respective analysis performed on the extract. The chromatogram, shown in Figure 4.3, reveals that the number of identified high molecular weight aromatic substances is reduced to six, significantly lower compared to the respective chromatogram of the pyrolysis process where 29 possible substances are identified. Naphthalene persists as one of the main compounds present in the final tar. The table below lists the possible substances identified.

Table 4-9 Substances trapped in cotton filter. TC

ID	Identification
1	Phenol
2	Naphthalene
3	Biphenylene
4	Phenanthrene
5	Fluoranthene
6	Pyrene
7	Eicosane

It is worth noting that the appearance or color of the cotton filter shows the existence or formation of some kind of soot, which for the purposes of this work will not be considered in the mass balance.

Of the substances listed in Table 4.9, (Vassilatos et al., 1992) reported all substances except phenol and eicosane for a thermal cracking process at 900°C.
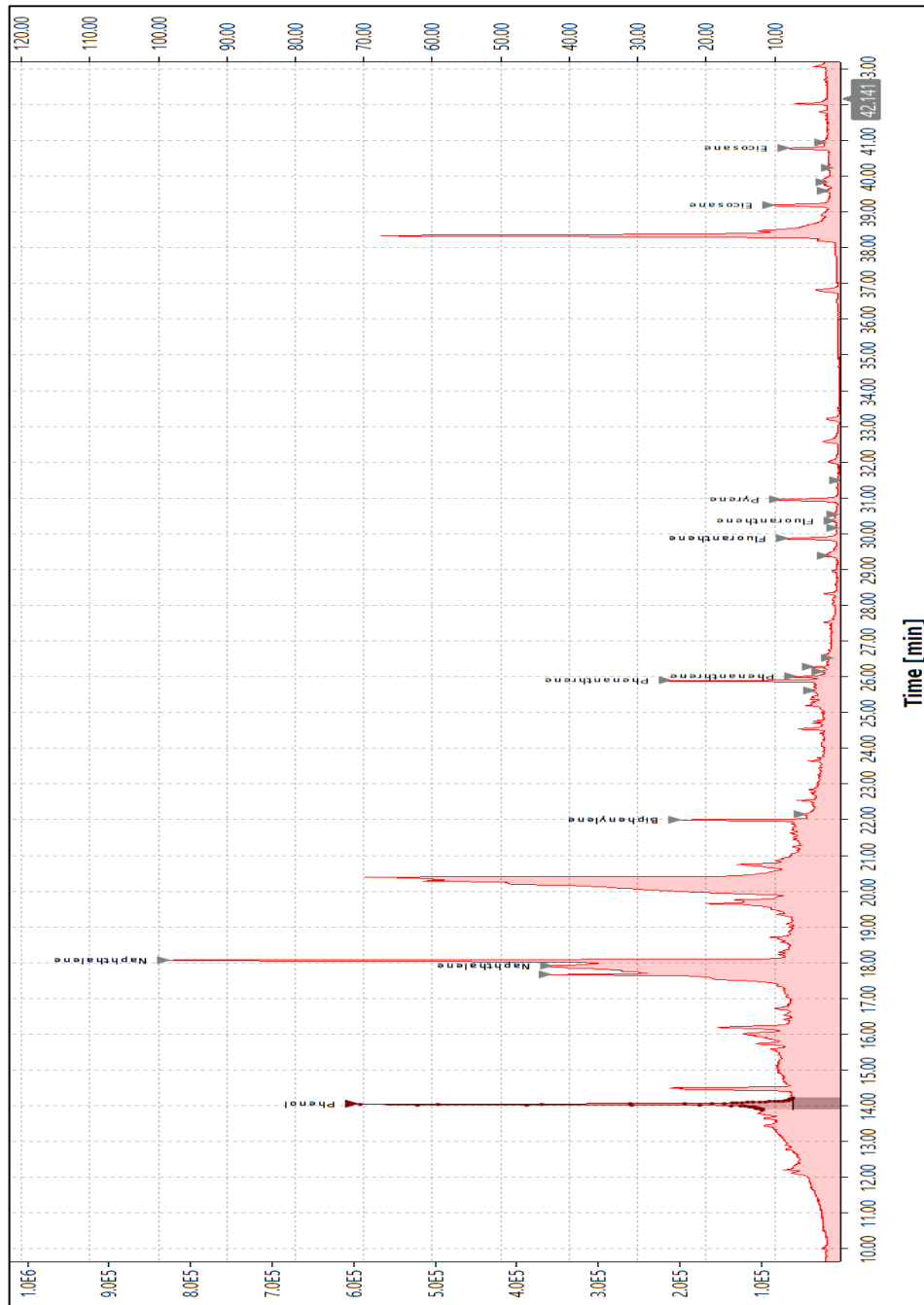
Figure 0-3 Chromatogram cotton filter. Thermal cracking

4.5 Thermal cracking baseline case

To facilitate a comparison between pyrolysis and thermal cracking, the data collected from cases TC02, TC02A, TC02B, and TC02C will be used to create an average thermal cracking case. Below are tables presenting the thermal cracking baseline data and a comparison with the pyrolysis baseline.

The substance CH_mO_n represents the new tar formed during the thermal cracking of large molecules present in the vapors from pyrolysis, into smaller molecules.

Table 4-10 Global mass balance for thermal cracking baseline

	Mass (g)	Gas	Molar fraction
Gases	**66.48**	H_2	0.2837
		CH_4	0.1355
		CO	0.3851
		CO_2	0.1652
		C_2H_4	0.0120
		C_2H_6	0.0005
		C_3H_6	0.0002
		C_3H_8	0.0178
	Mass (g)	**Substances**	**Mass fraction**
Final tar – water	**15.32**	Water + CH_mO_n	

The graphical representation of the thermal cracking material balance process is
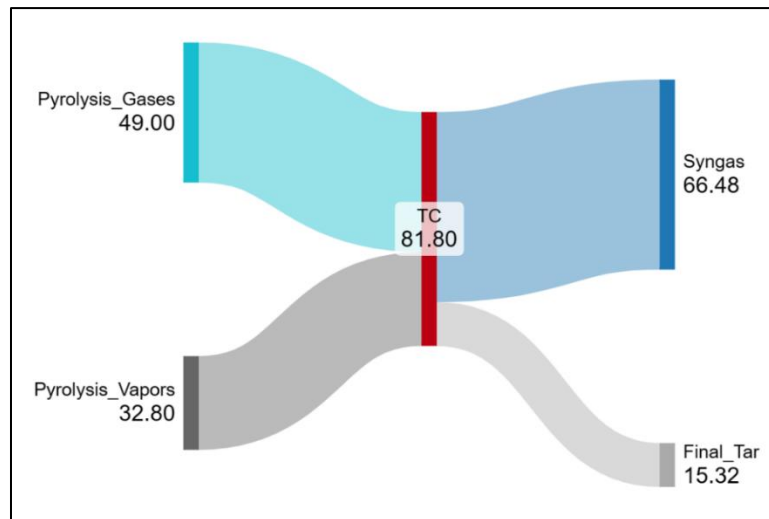
Figure 0-4 Graphical representation of TC mass balance 100 g biomass

Table 4-11 Net mass production of gases. Comparison PRBC-TCBC

	g/100 g Biomass	
Gas	PRBC	TCBC
H_2	0.384	1.720
CH_4	3.955	6.572
CO	22.722	32.688
CO_2	16.881	22.036
C_2H_4	1.391	1.019
C_2H_6	0.916	0.045
C_3H_6	0.917	0.025
C_3H_8	1.257	2.374
C_4H_{10}	0.576	0.000

The same data will be show in term of mole to do the respective mass balance.

Table 4-12 Net mole production/consumption comparison PRBC-TCBC

	mole/100 g biomass		
Gas	PRBC	TCBC	Net mole produced
H_2	0.1920	0.8600	0.6680
CH_4	0.2472	0.4108	0.1636
CO	0.8115	1.1674	0.3559
CO_2	0.3837	0.5008	0.1172
C_2H_4	0.0497	0.0364	-0.0133
C_2H_6	0.0305	0.0015	-0.0290
C_3H_6	0.0218	0.0006	-0.0212
C_3H_8	0.0286	0.0540	0.0254
C_4H_{10}	0.0099	0.0000	-0.0099

The cracking of C_2-C_4 mixtures was studied by (Sundaram & Froment, n.d.), the reactions involved in the cracking process are summarized in Table 4.13. As a first step in the results analysis, the mixture of gas from the pyrolysis reactor along with steam and vapors will be simulated using the reaction scheme. The analysis is conducted using an equilibrium reactor, where all the reactions are introduced. Subsequently, the mathematical model minimizes the Gibbs free energy to calculate the composition at equilibrium. It's important to clarify that this is an approximation and provides the maximum conversion of the respective substances without any kinetic analysis.

However, this analysis is important because it demonstrates the thermodynamic limitations of the chemical reactions involved in the cracking process.

Table 4-13 Cracking model for C_2-C_4 mixtures.

ID	Reaction
1	$C_2H_6 \rightarrow C_2H_4 + H_2$
2	$2C_2H_6 \rightarrow C_3H_8 + CH_4$
3	$C_2H_4 + C_2H_6 \rightarrow C_3H_6 + CH_4$
4	$C_3H_8 \rightarrow C_3H_6 + H_2$
5	$C_3H_8 \rightarrow C_2H_4 + CH_4$
6	$C_3H_8 + C_2H_4 \rightarrow C_2H_6 + C_3H_6$
7	$2C_3H_6 \rightarrow 3C_2H_4$
8	$C_4H_{10} \rightarrow C_3H_6 + CH_4$
9	$C_4H_{10} \rightarrow 2C_2H_4 + H_2$
10	$C_4H_{10} \rightarrow C_2H_4 + C_2H_6$
11	$C_3H_6 + H_2 \rightarrow C_2H_4 + CH_4$

The K_{eq} values correspond to the equilibrium constant calculated according to the definition:

$$K_{eq} = \frac{\prod[Products]}{\prod[Reactants]}$$

23

The K_{eq} for each one of the reactions is tabulated in table 4.14.

Table 4-14 K_{eq} calculated for C_2-C_4 thermal cracking model

ID	Reaction	K_{eq} Calculated @ 950 °C
1	$C_2H_6 \rightarrow C_2H_4 + H_2$	8.544
2	$2C_2H_6 \rightarrow C_3H_8 + CH_4$	3.234
3	$C_2H_4 + C_2H_6 \rightarrow C_3H_6 + CH_4$	18.860
4	$C_3H_8 \rightarrow C_3H_6 + H_2$	49.823
5	$C_3H_8 \rightarrow C_2H_4 + CH_4$	2876.592
6	$C_3H_8 + C_2H_4 \rightarrow C_2H_6 + C_3H_6$	5.832
7	$2C_3H_6 \rightarrow 3C_2H_4$	26.155
8	$C_4H_{10} \rightarrow C_3H_6 + CH_4$	16635.730
9	$C_4H_{10} \rightarrow 2C_2H_4 + H_2$	7536.142
10	$C_4H_{10} \rightarrow C_2H_4 + C_2H_6$	882.060
11	$C_3H_6 + H_2 \rightarrow C_2H_4 + CH_4$	57.736

The second approach is a kinetic model, where the rate of production for a component A is given by:

$$-r_A = k * f([Concentrations])$$ 24

$$k = k_0 * exp^{\left(\frac{-E_a}{R*T}\right)}$$ 25

The respective data to implement the kinetic model is tabulated next:

Table 4-15 Kinetic parameters for C_2-C_4 thermal cracking model

ID	Reaction	k_0	E_a (kcal/mole)
1	$C_2H_6 \rightarrow C_2H_4 + H_2$	4.65E+13	65.21
2	$2C_2H_6 \rightarrow C_3H_8 + CH_4$	3.75E+12	65.25
3	$C_2H_4 + C_2H_6 \rightarrow C_3H_6 + CH_4$	7.08E+13	60.43
4	$C_3H_8 \rightarrow C_3H_6 +H_2$	5.89E+10	51.29
5	$C_3H_8 \rightarrow C_2H_4 +CH_4$	4.69E+10	50.60
6	$C_3H_8 + C_2H_4 \rightarrow C_2H_6 + C_3H_6$	2.54E+13	59.06
7	$2C_3H_6 \rightarrow 3C_2H_4$	1.51E+11	55.80
8	$C_4H_{10} \rightarrow C_3H_6 + CH_4$	7.00E+13	59.64
9	$C_4H_{10} \rightarrow 2C_2H_4 + H_2$	7.00E+14	70.68
10	$C_4H_{10} \rightarrow C_2H_4 + C_2H_6$	4.10E+12	61.31
11	$C_3H_6 + H_2 \rightarrow C_2H_4 + CH_4$	5.77E+09	35.00

Now, taking in consideration ONLY the C_2-C_4 thermal cracking reactions, the net mole in the syngas stream, calculated using both approaches is shown below:

Table 4-16 Final mole in stream comparison equilibrium-kinetic

	mole/100 g biomass	
	Equilibrium	Kinetic
H_2	0.1532	0.2308
CH_4	0.3540	0.2772
C_2H_4	0.1145	0.1606
C_2H_6	0.0008	0.0000
C_3H_6	0.0046	0.0000
C_3H_8	0.0000	0.0000
C_4H_{10}	0.0000	0.0000

At this point, it's important to clarify that the thermal cracking of C_2-C_4 has been considered alone. The next step is to introduce the thermal cracking of vapors to complete the mass balances. Treating the vapor mixture as the surrogate and considering the results from the C_2-C_4 cracking model along with the mass balance, the decomposition of the vapors is given by:

53

$$CH_yO_z + \Delta H_2O \rightarrow \alpha CO + \beta CO_2 + \gamma CH_4 + \delta H_2 + \sigma CH_mO_n$$

According to the PRBC, the chemical formula surrogate is given by $CH_{2.27}O_{0.59}$. Taking 100 g of biomass and the molecular structure for the surrogate the mole of surrogate generated is:

Surrogate	MW	mass/100 g biomass	mole/100 g biomass
$CH_{2.27}O_{0.59}$	23.71 g/mol	17.017 g	0.7177

With this information linked to the experimental mass balance, the reaction takes the next form, in the case of 100 g biomass.

$$0.7177CH_{2.27}O_{0.59} + \Delta H_2O \rightarrow \alpha CO + \beta CO_2 + \gamma CH_4 + \delta H_2 + \sigma CH_mO_n$$
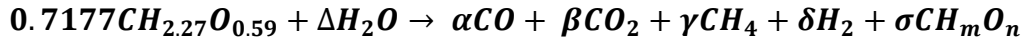
The values α and β are calculated from the difference between TCBC and PRBC regarding the components CO and CO_2. Those values are:

$$\alpha: 0.3559 \qquad \beta: 0.1172$$
$$0.7177CH_{2.27}O_{0.59} + \Delta H_2O \rightarrow 0.3559CO + 0.1172CO_2 + \gamma CH_4 + \delta H_2 + \sigma CH_mO_n$$
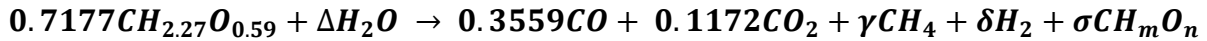
The stochiometric coefficients γ and δ, are calculated linking the experimental mass balance and the kinetic thermal cracking for the mixture C_2-C_4, using the PFR reactor in Aspen Plus together the specification designs to meet the experimental values, the preliminary thermal decomposition model for the surrogate is:

$$0.7177CH_{2.27}O_{0.59} + \Delta H_2O$$
$$\rightarrow 0.3559CO + 0.1172CO_2 + 0.1283CH_4 + 0.6345H_2 + \sigma CH_mO_n$$
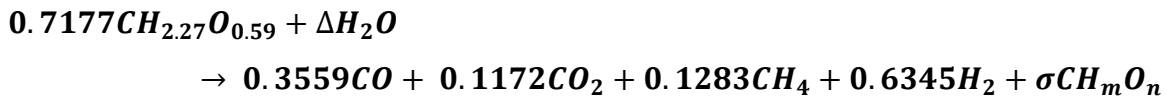
The value for the coefficient σ is found from the carbon balance:

$$\sigma = 0.7177 - 0.3559 - 0.1172 - 0.1283 = 0.1163$$

Thus, the partial model is:

$$0.7177CH_{2.27}O_{0.59} + \Delta H_2O$$
$$\rightarrow 0.3559CO + 0.1172CO_2 + 0.1283CH_4 + 0.6345H_2 + 0.1163CH_mO_n$$
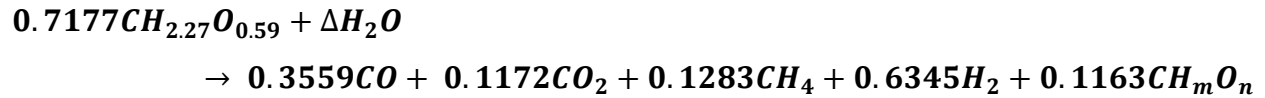
The remaining atomic balances, Hydrogen and Oxygen are related with the parameters Δ, m and n, according to:

- ➤ Hydrogen Balance:
$$0.7177 * 2.27 + 2\Delta = 4 * 0.1283 + 2 * 0.6345 + 0.1163m$$
- ➤ Oxygen balance:
$$0.7177 * 0.59 + \Delta = 0.3559 + 2 * 0.1172 + 0.1163n$$

The stoichiometric coefficients m and n as a function of the parameter Δ have the next expression:
$$m = \frac{2\Delta - 0.1530}{0.1163}$$
$$n = \frac{\Delta - 0.1669}{0.1163}$$

Under the assumption that all the oxygenated compounds present in the vapors coming from pyrolysis are cracked, the value for n should be "0" implying the next:
$$n = 0$$
$$\Delta = 0.1669$$
$$m = 1.5546$$

Under those assumptions, the model for the thermal cracking for the vapors is:

$$0.7177CH_{2.27}O_{0.59} + 0.1669H_2O$$
$$\rightarrow 0.3559CO + 0.1172CO_2 + 0.1283CH_4 + 0.6345H_2$$
$$+ 0.1163CH_{1.5546}$$
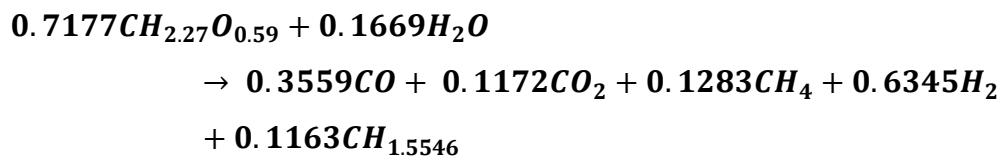
Or, for a clearer way to visualize the balance:

$$CH_{2.27}O_{0.59} + 0.2325H_2O$$
$$\rightarrow 0.4959CO + 0.1633CO_2 + 0.1788CH_4 + 0.8841H_2$$
$$+ 0.1620CH_{1.5546}$$

It is important to clarify that the model proposed earlier is a special case where all the oxygenated substances originally present in the vapors have been converted into H_2, CO, and substances composed of C and H. The most probable scenario, according to the observation of the condensed tar at the end of the thermal cracking process, shows that there are still oxygenated substances in the tar. Obviously, this could be verified with respective analyses of the bio-oil, such as HPLC and GC-MS, which were not carried out for the purposes of this work, as the composition and yield of the syngas are the main objectives.

The final model for the tar decomposition, according to the experimental data and adjusting the net amounts of man gases (H_2, CH_4, CO and CO_2) as the substances with the greatest mass percentage, and considering remaining oxygenated species in the final tar, is expressed as

$$CH_{2.27}O_{0.59} + \Delta H_2O$$
$$\rightarrow 0.4959CO + 0.1633CO_2 + 0.1788CH_4 + 0.8841H_2 + 0.1620CH_mO_n$$
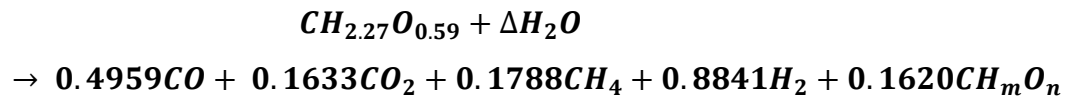
The values for the parameters Δ, m and n, are tabulated below:

Table 4-17 Coefficients for final tar as a function of water involved in cracking reaction

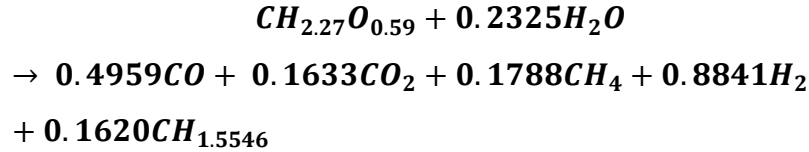| Δ	m	n
0.2325	1.5531	0.0000
0.2400	1.6457	0.0463
0.2500	1.7691	0.1080
0.2600	1.8926	0.1698
0.2700	2.0160	0.2315

It is very important to note that the value 0.2325 corresponds to the minimum value, according to the model proposed, that the parameter Δ can take, otherwise, the coefficient n will take a negative value, being this something incorrect in terms of stoichiometric coefficients and mass balance.

Introducing the vapor thermal cracking and the kinetic model for the thermal cracking of C_2-C_4 mixtures in Aspen Plus, with the respective data regarding to the reactor and flows, the results are show below. The assumption for the model implemented in Aspen Plus, for just the purpose to evaluate the decomposition of the mixture C_2-C_4, follows the next steps:

I.   Tar decomposition according to the respective model proposed.

II. The remaining gas and vapors mixture is cracked in a PFR following the kinetic model for C_2-C_4 thermal cracking depicted in table 4-15.

The result of the model is summarized below.

Table 4-18 Experimental and simulation results comparison for TC

	mole/100 g biomass	
	Experimental	Simulation cracking/kinetic model
H_2	0.8600	0.8601
CH_4	0.4108	0.4107
CO	1.1674	1.1674
CO_2	0.5008	0.5008
C_2H_4	0.0364	0.1579
C_2H_6	0.0015	0.0000
C_3H_6	0.0006	0.0000
C_3H_8	0.0540	0.0000
C_4H_{10}	0.0000	0.0000

The final tar collected will consist of several species, some of them could belong to the same species indicated in table 3.17. Just as an example, if the value Δ takes the value 0.2500, the Thermal Cracking model adopts the next form:

$$CH_{2.27}O_{0.59} + 0.2500H_2O$$
$$\rightarrow 0.4959CO + 0.1633CO_2 + 0.1788CH_4 + 0.8841H_2$$
$$+ 0.1620CH_{1.7691}O_{0.1080}$$
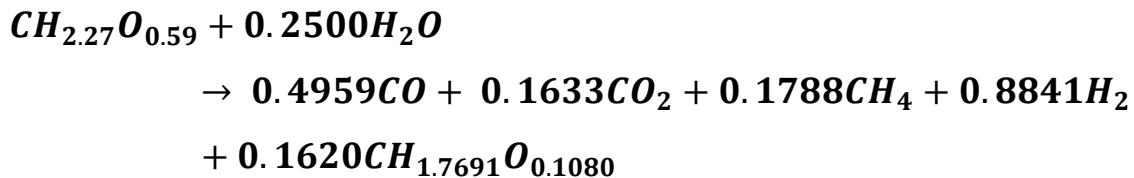
The final composition of the tar (as a surrogate) is:

$$CH_{1.7691}O_{0.1080}$$
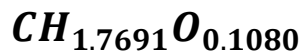
The mass balance is the tool that allows generating different molecular formulas for the surrogate, which in turn will be related to a composition different from the initial one, where a change in the appearance of the original bio-oil can be observed, transitioning from a highly viscous substance to a type of emulsion with lower viscosity than the original bio-oil.

Some of the possible species still present in the final tar (condensable fraction) could be:

Table 4-19 Some of the species probably present in tar

Name	C	H	O
Cresol	1	1.143	0.143
Heavy molecular lignin	1	1.167	0.167
Acrolein	1	1.333	0.333
Xylofuranose	1	1.600	0.800
Levoglucosan	1	1.667	0.833
Linalyl propionate	1	1.692	0.154
Methyl Linoleate	1	1.789	0.105

(Vassilatos et al., 1992), in his study on thermal cracking at 900 °C, observed an increase of 1.14 times the original amount of H_2, 1.25 times for CH_4, 1.33 times for CO, and finally 1.2 times the final amount of CO_2 in the gas subjected to thermal cracking. In the present study, the H_2 amount is 4.48 times the initial quantity, while the factors of increase for CH_4, CO, and CO_2 are 1.66, 1.43, and 1.31 respectively. It is important to clarify that in the present study, the operating temperature is 950 °C.

In a more recent study (Neves et al., 2011), a series of data on the respective yields of biochar and gas composition has been collected, analyzed, and graphed. Considering the peak temperature of the pyrolysis process, some studies reported that the ratio of kg-H_2/kg-CO in the gas, at a temperature of 1000 °C, is 0.055, a value very similar to the one obtained here, 0.053. It is noteworthy that the graph shows a linear increase between 400 °C and 600 °C, reaching a limit near 800 °C, where other points in the graph show ratios very close at 800 °C and 900 °C.

(Morf et al., n.d.) reported that in a homogeneous thermal cracking process, the H_2 yield was 7.4 times at 990 °C compered with the initial pyrolysis gas and the CO is the double when the temperature rises form 680 °C to 1000 °C.

The stoichiometric-kinetic model here proposed fix with the experimental data being important the water as reactant. (Boroson et al., n.d.) reported how the yield water went down from 16.3% (pyrolysis process) to 15.2% (thermal cracking at 1073 K).

Chapter 5

5 Catalytic cracking (CC)

For the catalytic cracking, there is a new definition:

$$WHSV \; (Weight \; Hourly \; Space \; Velocity)$$
$$= \frac{Mass \; Flow \; Rate \; IN \; (Gases + Vapors)}{Catalyst \; mass} \left[\frac{g/h}{g} = h^{-1} \right] \qquad 26$$

5.1 Operating Conditions

The table 5.1 shows the conditions for each one of the experiments done using the catalyst prepared according to the explained in chapter 2. The reactor used correspond to the same used in the case of thermal cracking, in this case was filled with the catalyst, and the vapors and gases were introduced following an ascending path inside the reactor.

Table 5-1 Operating conditions and final tar CC

	Temperature (K)	Pressure (psig)	WHSV (h^{-1})	Final tar collected (% biomass)
CC01			0.785	14.17%
CC02			0.534	14.09%
CC03	1223	1.0	0.205	14.42%
CC04			0.177	13.49%
CC05			0.146	13.40%

5.2 Gas compositions

The respective syngas composition is tabulated below:

Table 5-2 Syngas compositions for CC

	CC01	CC02	CC03	CC04	CC05
H$_2$	29.60%	29.55%	36.92%	37.35%	37.91%
CH$_4$	14.65%	14.64%	10.04%	8.16%	7.42%

CO	37.91%	38.94%	44.41%	47.38%	48.66%
CO$_2$	14.44%	13.94%	8.13%	6.95%	5.99%
C$_2$	3.40%	2.93%	0.50%	0.16%	0.03%

It is important to note that the component C$_2$ in table 5.2, corresponds to the species C$_2$H$_4$ and C$_2$H$_6$, the experiments using the catalyst didn't show C$_3$H$_6$ or C$_3$H$_8$.

To evaluate the performance of the olivine catalyst utilized in this study, a comparison was conducted with results reported by other researchers. The table below presents the respective values. It's worth noting that the results depicted here pertain specifically to catalytic reforming of vapors and gases obtained through pyrolysis, excluding gasification processes.

Table 5-3 Syngas composition. Comparison of different catalyst

			SYNGAS Composition			
Work	**Catalyst**	**Temp. (ºC)**	**H$_2$**	**CH$_4$**	**CO**	**CO$_2$**
Present work CC05	Olivine	950	37.9%	7.4%	48.7%	6.0%
(Abou Rjeily, Chaghouri, et al., 2023)	Nickel	800	41.1%	5.1%	39.0%	13.8%
(Raymundo et al., 2019)	Zeoilte	700	22.8%	11.8%	50.1%	10.4%

5.3 Yields

The composition and the yields are used to calculate the respective net mass for each one of the species, showing the results in the table below.

Table 5-4 Gases net production. CC

	g / 100 g biomass				
	CC01	**CC02**	**CC03**	**CC04**	**CC05**
H$_2$	1.92	1.92	2.69	2.77	2.85
CH$_4$	7.60	7.63	5.85	4.84	4.46
CO	34.42	35.50	45.29	49.19	51.17
CO$_2$	20.60	19.97	13.03	11.34	9.90
C$_2$	3.09	2.68	0.52	0.17	0.03

To make a comparison of the results, the data from experiment CC05 will be taken as the best result achievable under the conditions given in table 5.1. The data in terms of mole is calculated and tabulated next:

Table 5-5 Comparison gases net mass production

Gas	mole/100 g biomass		
	PRBC	TCBC	CC05
H_2	0.1920	0.8600	1.4235
CH_4	0.2472	0.4108	0.2786
CO	0.8115	1.1674	1.8273
CO_2	0.3837	0.5008	0.2249
C_2H_4	0.0497	0.0364	0.0011
C_2H_6	0.0305	0.0015	0.0000
C_3H_6	0.0218	0.0006	0.0000
C_3H_8	0.0286	0.0540	0.0000
C_4H_{10}	0.0099	0.0000	0.0000

The results in table 5.5. suggest the CO2 is reacting with other species. This reaction is known as "dry reforming", and this could explain why the CO_2 content is lower for the CC experiments.

5.4 Final tar and PAH

The qualitative analysis of the tar collected from the catalytic reforming of pyrolysis vapors reveals crucial insights into the chemical transformations occurring during the process. Figure 5.1 illustrates the composition of the final tar, showcasing a notable enhancement in the reforming and cracking of the original bio-oil constituents. This observation suggests effective catalytic activity leading to the decomposition of complex organic molecules into lighter hydrocarbons and gaseous products, indicative of successful reforming processes.

However, despite the favorable reforming outcomes, the qualitative assessment also identifies the presence of residual heavy hydrocarbon compounds within the final tar fraction. These compounds contribute to the turbidity observed in the tar, indicating incomplete conversion or partial cracking of certain high molecular weight species.
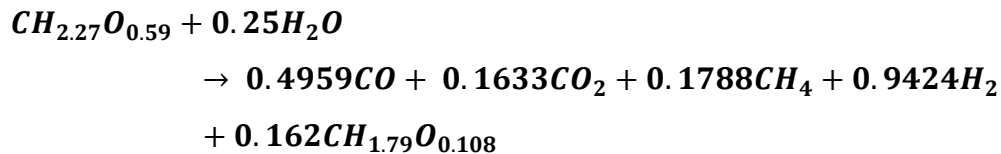
Figure 0-1 Final tar. CC


Figure 0-2 PAH trapped in cotton filter. CC

5.5 Catalytic cracking model

Considering the mass balance, the yields obtained, and taking the base case of pyrolysis, along with the data from case CC05, the following model is proposed to represent thermal cracking, which can be understood as a special case of reforming because water is part of the model. Next is the expression for the catalytic cracking model.

$$CH_{2.27}O_{0.59} + 0.25H_2O$$
$$\rightarrow 0.4959CO + 0.1633CO_2 + 0.1788CH_4 + 0.9424H_2$$
$$+ 0.162CH_{1.79}O_{0.108}$$

In this model, the stoichiometric coefficient belonging to the hydrogen has been modified to close the atomic balance, and the same for the atomic formula belonging to the final tar, specifically the value for the oxygen, however this value is very similar to the original proposed for the methyl linoleate as the main component in the final tar collected.

The study done by (Shah & Gardner, 2014) regarding the dry reforming of methane and ethylene, follows the next scheme:

$$CH_4 + CO_2 \rightarrow 2CO + 2H_2$$
$$C_2H_4 + 2CO_2 \rightarrow 4CO + 2H_2$$
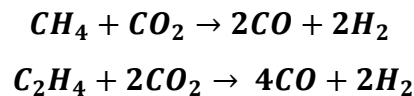
Several author (Shah & Gardner, 2014), (Kryca et al., 2018), (Quan et al., 2017), who worked with olivine as catalyst for tar removal, implemented in their models WGSR as a fundamental reaction

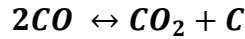taking pace in the cracking or reforming of the components content in the pyrolysis vapors. The reaction is described next:

$$CO + H_2O \leftrightarrow CO_2 + H_2$$
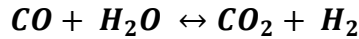
Another reaction to consider is the Boudouard reaction, represented by:

$$2CO \leftrightarrow CO_2 + C$$

However, in their work (Wu & Liu, 2010), showed that in the catalytic reforming of bio-oil using cresol as a model component, the carbon elimination reaction is present and is represented by:

$$C + H_2O \rightarrow H_2 + CO$$
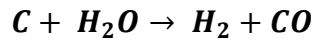
In tis same work, Wu & Liu show that carbon deposition on the catalyst surface increases with temperature, reaching a peak at 750°C. Subsequently, it diminishes following a pattern reminiscent of its initial ascent, eventually reaching a value as low at 900°C as it does at 600°C.

The proposed catalytic cracking model is constructed as a series of processes described below, with numerical values derived for a baseline case of 100 grams of biomass. The model comprises three main steps:

➢ Vapors and gases from pyrolysis are cracked following a stoichiometric model

Table 5-6 Input-output stoichiometric cracking. 100 g biomass

INPUT			OUTPUT	
Vapors & gases PRBC	Mole		Gases & vapors	Mole
H_2	0.1920	First step catalytic cracking model	H_2	0.8684
CH_4	0.2472		CH_4	0.3755
CO	0.8115		CO	1.1674
CO_2	0.3837		CO_2	0.5009
C_2H_4	0.0497		C_2H_4	0.0497
C_2H_6	0.0305		C_2H_6	0.0305
C_3H_6	0.0218		C_3H_6	0.0218
C_3H_8	0.0286		C_3H_8	0.0286
C_4H_{10}	0.0099		C_4H_{10}	0.0099
$CH_{2.27}O_{0.59}$	0.7177		$CH_{1.79}O_{0.108}$	0.1620

➢ Kinetic thermal cracking model for C_2-C_4 mixtures

Table 5-7 Input-output kinetic cracking model C_2-C_4 mixtures. 100 g biomass

INPUT			OUTPUT	
Gases	**Mole**		**Gases**	**Mole**
H_2	0.8684		H_2	0.9020
CH_4	0.3755	**Second step**	CH_4	0.4109
CO	1.1674	**kinetic**	CO	1.1674
CO_2	0.5009	**cracking C_2-**	CO_2	0.5009
C_2H_4	0.0497	**C_4 Table**	C_2H_4	0.1580
C_2H_6	0.0305	**4.15**	C_2H_6	0.0000
C_3H_6	0.0218		C_3H_6	0.0000
C_3H_8	0.0286		C_3H_8	0.0000
C_4H_{10}	0.0099		C_4H_{10}	0.0000

The difference between the model proposed in the chapter on thermal cracking and the model proposed here, lies in the stoichiometric coefficients for the species involve and, for the special case of catalytic cracking, the dry reforming process added to fit the experimental data.

➢ Dry reforming of CH_4 and C_2H_4 and WGSR

Table 5-8 Input-output dry reforming of methane and ethylene. 100 g biomass

INPUT			OUTPUT	
Gases	**Mole**		**Gases**	**Mole**
H_2	0.9020		H_2	1.4344
CH_4	0.4109		CH_4	0.3046
CO	1.1674	**Third step dry**	CO	1.8207
CO_2	0.5009	**reforming CH_4**	CO_2	0.2074
C_2H_4	0.1580	**and C_2H_4**	C_2H_4	0.0313
C_2H_6	0.0000	**and WGSR**	C_2H_6	0.0000
C_3H_6	0.0000		C_3H_6	0.0000
C_3H_8	0.0000		C_3H_8	0.0000
C_4H_{10}	0.0000		C_4H_{10}	0.0000

With the experimental data and solving the model to find the minimum value for the square of the error, the model could be solve using the definition given by (Smith et al., n.d.), about reaction coordinate. The definition is:

$$\int_{n_{i0}}^{n_i} dn_i = v_i \int_0^{\varepsilon} d\varepsilon \qquad\qquad 27$$

Where:

n_i: mole of substance i

v_i: stoichiometric coefficient for substance i ((+) for products, (-) for reactants)

ε: reaction coordinate.

In the case of multiple reactions, the final amount of the substance i is calculated as follows:

$$n_i = n_{i0} + \sum_{j=1}^{r} v_{i,j}\varepsilon_j \qquad\qquad 28$$

r: is the number of reactions and j is used to identify each one of the reactions.

The model to be developed consists of finding the respective stoichiometric coefficients in the cracking model of the bio-oil model substance and the reaction coordinates of the dry reforming reactions.

During the experimental part and subsequent analyses of the catalyst regarding the initial and final weight deposited in the reactor, no increase in the catalyst's weight was detected, and therefore, the carbon decomposition reaction will not be considered.

The results are summarized in table 5.9.

Table 5-9 Difference experimental - models CC

Gases	Mole / 100 g biomass		
	Experimental	Three step model for catalytic cracking	Difference mole/100 g biomass
H_2	1.4235	1.4344	0.0109
CH_4	0.2786	0.3046	0.0260
CO	1.8273	1.8207	-0.0066
CO_2	0.2249	0.2074	-0.0175
C_2H_4	0.0011	0.0313	0.0302
C_2H_6	0.0000	0.0000	0.0000
C_3H_6	0.0000	0.0000	0.0000

C_3H_8	0.0000	0.0000	0.0000
C_4H_{10}	0.0000	0.0000	0.0000

Chapter 6

6 Catalytic steaming (CS)

For the CS, there is a new definition:

$$WHSV_s \ (Weight \ Hourly \ Space \ Velocity - Steaming)$$
$$= \frac{Mass \ Flow \ Rate \ IN \ (Gases + Vapors + Steam)}{Catalyst \ mass} \left[\frac{g/h}{g} = h^{-1} \right]$$

6.1 Operating Conditions

The table 6.1 shows the conditions for each one of the experiments. The preparation of the catalyst follows the same guidelines explained in chapter 2. The steam used in this case was generated using a ¼" stainless steel tube, coiled around the PBR reactor. The total length of the tube was 3 m. The steam was injected into the reactor before the vapors and gases coming from the pyrolysis reactor, into a hot zone. The mixing zone (Steam – Vapors) has a volume of 200 cm^3, below the packed volume.

Table 6-1 Operating conditions for CS experiments

	Temperature (K)	Pressure (psig)	WHSV (h^{-1})	Steam/biomass (g/g)	S/C (mole H$_2$O/mole C V&G)
CS01			0.430	0.90	2.00
CS02			0.370	0.90	2.01
CS03	1223	1.0	0.270	0.70	1.58
CS04			0.154	0.72	1.60
CS05			0.122	0.72	1.60

Some of the Reported conditions reported are listed below.

Table 6-2 Selected operating conditions reported. Steam reforming of vapors from pyrolysis

	Temp.	WHSV (h^{-1})	S/C (mole H$_2$O/mole C V&G)
(Quan et al., 2017)	800 ºC	0.500	2.00
(Wu & Liu, 2010)	900 ºC	NA	1.86
(D. Wang et al., 1997)	850 ºC	NA	5.10
(Arregi et al., 2016)	600 ºC	0.200	4.00

6.2 Syngas composition

The composition of the Syngas reported below for each of the experiments corresponds to the arithmetic average of the composition analyzed using the micro-GC analyzer, for each of the samples taken during the duration of the experiment.

Table 6-3 Syngas composition. CS

	Syngas composition				
	CS01	CS02	CS03	CS04	CS05
H_2	46.81%	46.57%	43.88%	45.20%	43.14%
CH_4	10.66%	10.77%	11.87%	11.08%	11.55%
CO	22.96%	18.64%	22.39%	22.67%	22.33%
CO_2	17.16%	21.60%	20.11%	18.90%	20.69%
C_2-C_3	2.41%	2.44%	1.74%	2.16%	2.28%

Table 6-4 Syngas compositions reported

	Syngas composition			
	H_2	CH_4	CO	CO_2
This work CS01	46.8%	10.7%	23.0%	17.2%
(Quan et al., 2017)	40.0%	15.0%	17.0%	25.0%
(Wu & Liu, 2010)	63.0%	0.4%	26.3%	16.1%
(Arregi et al., 2016)	65.0%	0.1%	4.0%	30.0%

6.3 Net gas production

The net amounts of each gas are calculated using the respective mass balance associated with the compositions of the gases and the biochar and yields. Table 6.5 shows these quantities in terms of grams of each gas per 100 grams of biomass fed into the process.

Table 6-5 Net gas mass production CS

	Net mass g gas/100 g biomass				
	CS01	CS02	CS03	CS04	CS05
H_2	3.8	3.8	3.4	3.5	3.1
CH_4	6.9	7.0	7.3	6.9	6.5
CO	26.2	21.2	24.0	24.6	22.1
CO_2	30.7	38.5	33.8	32.2	32.2
C_2-C_3	3.1	3.1	2.1	2.7	2.7

With the composition data of the original biomass and the baseline case provided in the pyrolysis chapter, the maximum amount of available hydrogen in the vapor and gas stream is given by the following expression:

$$H_2^{max} = 100 * 0.0569 - 18.2 * 0.028 = 5.18 \; ^{g \; H_2}/_{100 \; g \; biomass}$$

Note that in the preceding expression, hydrogen content in the biomass on a DAF basis is considered. Therefore, hydrogen content in the initial moisture is not accounted for in this calculation. With this value, it is possible to calculate a percentage of hydrogen extracted from the original biomass for each of the processes evaluated here (pyrolysis, TC, CC, CS). The following table shows this percentage.

Table 6-6 Hydrogen extraction for each process studied

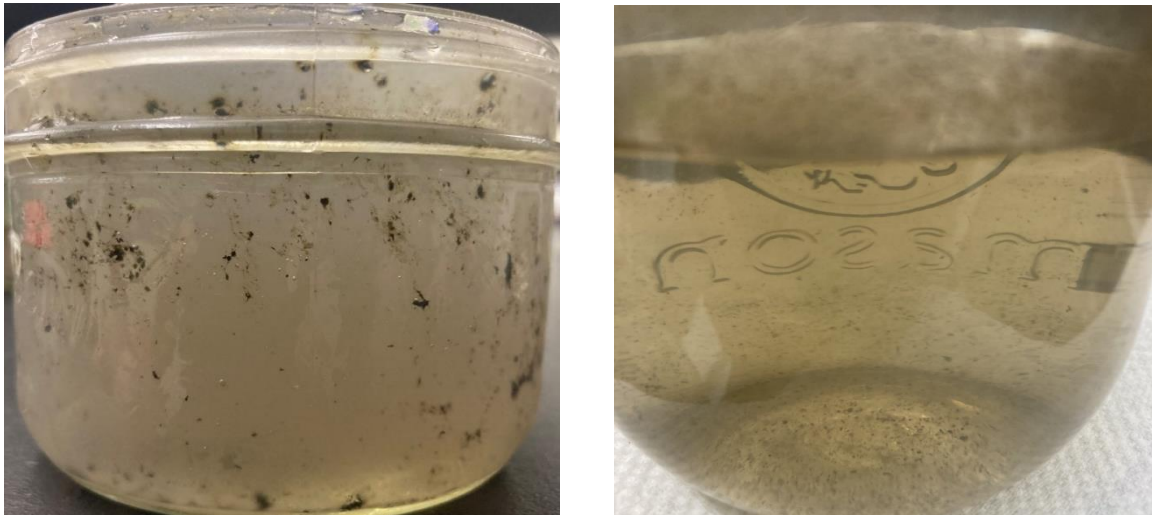|	g H$_2$ / 100 g biomass	% extracted H$_2$
PRBC	0.384	7.4%
TCBC	1.720	33.2%
CC05	2.850	55.0%
CS01	3.810	73.6%

6.4 Final tar and PAH

Figure 0-1 Final tar collected in CS

Figure 0-2 PAH trapped in cotton filter. CS

The figures 6.1 and 6.2 related to the collected final tar and the visual appearance of the cotton filter demonstrate the synergistic effect of the catalyst and steam injection into the reactor, allowing for the following beneficial effects:

➢ Apparent cracking of virtually all high molecular weight hydrocarbons present in the vapors, evidenced by a nearly transparent collected final tar.

➢ The cracking or reforming of PAH and their conversion into gases such as H_2 and CO.

To conclude, the composition of the final gas is tabulated below for the four main gases H_2, CH_4, CO, and CO_2 in terms of total mass, for comparison.

Table 6-7 Net mass in syngas stream comparison

	g/100 g biomass			
	PRBC	**TCBC**	**CC05**	**CS01**
H_2	0.38	1.72	2.85	3.81
CH_4	3.96	6.57	4.46	6.94
CO	22.72	32.69	51.17	26.16
CO_2	16.88	22.04	9.90	30.73

Table 6.7 demonstrates the complexity of the reforming mechanism involved for the hydrocarbons present in the pyrolysis vapors and the subsequent reactions that can take place among the gases or light molecules generated by this process. Undoubtedly, the increase in the quantity of

71

Hydrogen produced is evident. Additionally, the experimental results show an increase in CH_4 and CO_2 alongside a consumption of CO. These gases are intrinsically related through reactions such as methane reforming, water-gas shift reaction (WGSR), methanation, Boudouard reaction, dry reforming, and the various reactions occurring in vapor reforming. For this reason, as it is beyond the scope of this work, a comprehensive reaction mechanism is not proposed.

Chapter 7

Conclusions and future work

7.1 Pyrolysis Conclusions

The pyrolysis process demonstrates great stability in terms of compositions and yields within a biomass feed range between 4 and 10 g/min, while keeping the biomass and temperature and pressure conditions constant. This allows the creation of a model or baseline case, in which the compositions of gases and vapors, in terms of their elemental composition, will be very close, achieving stable conditions in the subsequent processes of thermal cracking and catalytic cracking.

The compositions of the gases obtained reflect what has been reported by other researchers and fall within the known ranges for this type of process, although it is difficult to find studies or reports on pyrolysis at the temperature selected for this work.

The biochar yield is within the reported range, as well as its elemental composition, being very consistent in every one of the experiments.

The gas and bio-oil yields showed the greatest discrepancy compared to what has been reported by different researchers, but it is worth noting that research on pyrolysis and its respective reports at temperatures above 500 degrees is very scarce. This is the point to discuss regarding the results obtained. However, since they are very close values for all experiments conducted, it is considered as the appropriate and true value for the selected working conditions.

7.2 Thermal Cracking

The thermal cracking process of gases and vapors demonstrates its effectiveness in increasing the net production of hydrogen by a ratio of approximately 4.48 times the initial amount present in the pyrolysis gas. Likewise, this determines that approximately 50% of the vapors or bio-oil are converted into gas. This is demonstrated by the yields of the final vapors collected, which in this work are treated as the final tar that is collected in the condensers. The yields show similar values, providing the certainty of an appropriate mass balance.

It is important to note that despite the H_2 concentrations in the syngas being on average 2.6 times higher for the selected operating conditions, the net quantity, in terms of grams or moles, is 4.48 times greater. A similar analysis should be conducted for the gases CO and CO_2, which despite showing a reduction in their concentration, the net quantity of these gases in the syngas stream is greater than in the gas stream generated in pyrolysis. This should be critically evaluated when assessing processes or research reports, as it becomes necessary to involve the respective yields or, in some cases, report the net quantities in terms of biomass or feedstock fed into the process.

The increase in the net quantity of CH_4, CO, CO_2 shows that, for this work and considering the hermeticity of the equipment used, the complete model of thermal cracking of the surrogate must include the generation of these gases and not simply the generation of H_2 and CO as shown in various studies.

The increase in the CH_4 substance is not only due to the thermal cracking of bio-oil but also part of the CH_4 is generated in the cracking process of the C_2-C_4 fraction mixture. Therefore, the balance of this substance involves a series of assumptions in the cracking mechanisms that may be susceptible to further studies.

The complete mechanism proposed in this work fits the experimental data to a good extent. The thermal cracking mechanism of the C_2-C_4 mixture is a reliable complete kinetic model that provides confidence in the proposed model. The point to review, due to lack of information and complete characterization of the bio-oil, would be the kinetics of thermal cracking for the surrogate, which in real terms should be modeled as a mixture of components. In the case of having kinetic data of thermal cracking, it could be coupled with the thermal cracking model of the C_2-C_4 mixtures to achieve complete mathematical modeling of the thermal cracking process.

The greatest difference in terms of gas concentration, which is the central theme of the work, was observed in the final concentration of the substance C_3H_8, which is still experimentally detected in the micro-GC, but according to the thermal cracking model, it should disappear. This could be due to several factors, including that the reported model may not be the best, or that C_3H_8 is generated in the vapor cracking process, and that it is indeed the substance that later generates CH_4.

Therefore, at the end of the process, downstream, it is formed but cannot be decomposed to generate more CH_4 and C_2H_4, as shown by the selected model.

7.3 Catalytic Cracking

The catalytic cracking process demonstrates its effectiveness in increasing the net quantity of H_2 in the syngas stream by a maximum factor of 7.414 times compared to the pyrolysis base case and 1.65 times compared to thermal cracking without a catalyst.

In the case of catalytic cracking, the decrease in the concentration of CO_2 and the respective mass balances do show a decrease in the net quantity of CO_2 in the syngas stream, which is important because in addition to achieving carbon capture by the biochar, its net content in the final syngas stream is reduced. The decrease in the quantity of CO_2 leads to proposing a dry reforming model as the most probable mechanism for its consumption in the process.

The thermodynamic analysis of the reactions involved in the dry reforming process reveals a favorable equilibrium constant at the operating temperature, suggesting a high probability of occurrence. However, the actual realization of these reactions is not guaranteed, as evidenced by the data from the thermal cracking case. This implies that the catalyst employed in this study, olivine, may demonstrate catalytic activity for the dry reforming process.

The proposed model for catalytic cracking of vapors and gases, involving slight modification of the stoichiometric coefficients of the surrogate cracking sub model and the addition of the dry reforming process, closely aligns for gases H_2, CH_4, CO, and CO_2, presenting the greatest deviations, like the thermal cracking case, in the gas C_2H_4.

The absence of C_3H_8 in the gas analysis of the syngas obtained through thermal cracking indicates significant cracking activity for the C_2-C_4 fraction originating from the pyrolysis gases.

The conversion of vapors to syngas using the catalyst, despite exhibiting higher conversion rates, must be considered alongside the fact that the final tar collected amounts to approximately 13%, representing a 2% in the conversion increase compared to the thermal cracking case. Noteworthy

is the qualitative assessment of the final tar, in catalytic cracking, it manifests as significantly more homogeneous, less viscous, and exhibits distinct characteristics from the tar collected in thermal cracking, as well as from the original bio-oil.

7.4 Catalytic Steaming

The qualitative and quantitative results demonstrate that the catalytic steaming increases the production of hydrogen in the gas stream, syngas. The increase is approximately 10 times compared to pyrolysis and 1.34 times compared to the use of the catalyst alone.

The injection of steam is very important to achieve the reforming of PAH, which is one of the major challenges in the management and subsequent utilization of gas obtained from the thermochemical transformation of biomass.

7.5 Future Work

The possibility of using olivine as a catalyst for the dry reforming process opens the doors for studying the utilization of CO_2 and its removal in the syngas stream.

The reaction mechanism of model compounds of bio-oil, using olivine as a catalyst, will help develop more precise mathematical models that allow simulation of the process and the respective optimization of parameters.

References

Abou Rjeily, M., Cazier, F., Gennequin, C., & Randrianalisoa, J. H. (2023). Detailed Analysis of Gas, Char and Bio-oil Products of Oak Wood Pyrolysis at Different Operating Conditions. *Waste and Biomass Valorization*, *14*(1), 325–343. https://doi.org/10.1007/s12649-022-01848-0

Abou Rjeily, M., Chaghouri, M., Gennequin, C., Abi Aad, E., Pron, H., & Randrianalisoa, J. H. (2023). Biomass Pyrolysis Followed by Catalytic Hybrid Reforming for Syngas Production. *Waste and Biomass Valorization*, *14*(8), 2715–2743. https://doi.org/10.1007/s12649-022-02012-4

Arregi, A., Lopez, G., Amutio, M., Barbarias, I., Bilbao, J., & Olazar, M. (2016). Hydrogen production from biomass by continuous fast pyrolysis and in-line steam reforming. *RSC Advances*, *6*(31), 25975–25985. https://doi.org/10.1039/c6ra01657j

Azeez, A. M., Meier, D., Odermatt, J., & Willner, T. (2010). Fast pyrolysis of African and European lignocellulosic biomasses using Py-GC/MS and fluidized bed reactor. *Energy and Fuels*, *24*(3), 2078–2085. https://doi.org/10.1021/ef9012856

Basu, P. (2010). Biomass Gasification and Pyrolysis. In *Biomass Gasification and Pyrolysis*. https://doi.org/10.1016/C2009-0-20099-7

Boroson, M. L., Howard, J. B., Longwell, J. P., & Peters, W. A. (n.d.). *Product Yields and Kinetics from the Vapor Phase Cracking of Wood Pyrolysis Tars*.

Brage, C., Yu, Q., & Sj6str6m, K. (1996). *Characteristics of evolution of tar from wood pyrolysis in a fixed-bed reactor* (Vol. 75, Issue 2).

Bridgwater, A. V. (2012). Review of fast pyrolysis of biomass and product upgrading. *Biomass and Bioenergy*, *38*, 68–94. https://doi.org/10.1016/j.biombioe.2011.01.048

Channiwala, S. A., & Parikh, P. P. (n.d.). *A unified correlation for estimating HHV of solid, liquid and gaseous fuels q*. http://www.fuel

Choi, Y. S., Johnston, P. A., Brown, R. C., Shanks, B. H., & Lee, K. H. (2014). Detailed characterization of red oak-derived pyrolysis oil: Integrated use of GC, HPLC, IC, GPC and Karl-Fischer. *Journal of Analytical and Applied Pyrolysis*, *110*(1), 147–154. https://doi.org/10.1016/j.jaap.2014.08.016

Debiagi, P. E. A., Gentile, G., Pelucchi, M., Frassoldati, A., Cuoci, A., Faravelli, T., & Ranzi, E. (2016). Detailed kinetic mechanism of gas-phase reactions of volatiles released from biomass pyrolysis. *Biomass and Bioenergy*, *93*, 60–71. https://doi.org/10.1016/j.biombioe.2016.06.015

Devi, L., Craje, M., Thüne, P., Ptasinski, K. J., & Janssen, F. J. J. G. (2005). Olivine as tar removal catalyst for biomass gasifiers: Catalyst characterization. *Applied Catalysis A: General*, *294*(1), 68–79. https://doi.org/10.1016/j.apcata.2005.07.044

Devi, L., Ptasinski, K. J., & Janssen, F. J. J. G. (2005). Pretreated olivine as tar removal catalyst for biomass gasifiers: Investigation using naphthalene as model biomass tar. *Fuel Processing Technology*, *86*(6), 707–730. https://doi.org/10.1016/j.fuproc.2004.07.001

Di Blasi, C. (2009). Combustion and gasification rates of lignocellulosic chars. In *Progress in Energy and Combustion Science* (Vol. 35, Issue 2, pp. 121–140). https://doi.org/10.1016/j.pecs.2008.08.001

Fredriksson, H. O. A., Lancee, R. J., Thüne, P. C., Veringa, H. J., & Niemantsverdriet, J. W. H. (2013). Olivine as tar removal catalyst in biomass gasification: Catalyst dynamics under model conditions. *Applied Catalysis B: Environmental*, *130–131*, 168–177. https://doi.org/10.1016/j.apcatb.2012.10.017

Fu, P., Yi, W., Li, Z., Bai, X., Zhang, A., Li, Y., & Li, Z. (2014). Investigation on hydrogen production by catalytic steam reforming of maize stalk fast pyrolysis bio-oil. *International Journal of Hydrogen Energy*, *39*(26), 13962–13971. https://doi.org/10.1016/j.ijhydene.2014.06.165

Kryca, J., Priščák, J., Łojewska, J., Kuba, M., & Hofbauer, H. (2018). Apparent kinetics of the water-gas-shift reaction in biomass gasification using ash-layered olivine as catalyst. *Chemical Engineering Journal*, *346*, 113–119. https://doi.org/10.1016/j.cej.2018.04.032

Kuhn, J. N., Zhao, Z., Felix, L. G., Slimane, R. B., Choi, C. W., & Ozkan, U. S. (2008). Olivine catalysts for methane- and tar-steam reforming. *Applied Catalysis B: Environmental*, *81*(1–2), 14–26. https://doi.org/10.1016/j.apcatb.2007.11.040

Marinkovic, J., Thunman, H., Knutsson, P., & Seemann, M. (2015). Characteristics of olivine as a bed material in an indirect biomass gasifier. *Chemical Engineering Journal*, *279*, 555–566. https://doi.org/10.1016/j.cej.2015.05.061

Morf, P., Hasler, P., & Nussbaumer, T. (n.d.). *Mechanisms and kinetics of homogeneous secondary reactions of tar from continuous pyrolysis of wood chips*. http://www.fuel

Mullen, C. A., Boateng, A. A., Hicks, K. B., Goldberg, N. M., & Moreau, R. A. (2010). Analysis and comparison of bio-oil produced by fast pyrolysis from three barley biomass/byproduct streams. *Energy and Fuels*, *24*(1), 699–706. https://doi.org/10.1021/ef900912s

Neves, D., Thunman, H., Matos, A., Tarelho, L., & Gómez-Barea, A. (2011). Characterization and prediction of biomass pyrolysis products. In *Progress in Energy and Combustion Science* (Vol. 37, Issue 5, pp. 611–630). Elsevier Ltd. https://doi.org/10.1016/j.pecs.2011.01.001

Palla, V. S. K. K., Papadikis, K., & Gu, S. (2015). A numerical model for the fractional condensation of pyrolysis vapours. *Biomass and Bioenergy*, *74*, 180–192. https://doi.org/10.1016/j.biombioe.2015.01.020

Quan, C., Xu, S., & Zhou, C. (2017). Steam reforming of bio-oil from coconut shell pyrolysis over Fe/olivine catalyst. *Energy Conversion and Management*, *141*, 40–47. https://doi.org/10.1016/j.enconman.2016.04.024

Radlein, D., Piskorz, J., & Scott, D. S. (1991). Fast pyrolysis of natural polysaccharides as a potential industrial process. In *Journal of Analytical and Applied Pyrolysis* (Vol. 19).

Rauch, R., Hofbauer, H., & Courson, C. (n.d.). *Comparison of different olivines for biomass steam gasification*. https://www.researchgate.net/publication/234834538

Raymundo, L. M., Mullen, C. A., Strahan, G. D., Boateng, A. A., & Trierweiler, J. O. (2019). Deoxygenation of Biomass Pyrolysis Vapors via in Situ and ex Situ Thermal and Biochar Promoted Upgrading. *Energy and Fuels*, *33*(3), 2197–2207. https://doi.org/10.1021/acs.energyfuels.8b03281

Shah, Y. T., & Gardner, T. H. (2014). Dry reforming of hydrocarbon feedstocks. *Catalysis Reviews - Science and Engineering*, *56*(4), 476–536. https://doi.org/10.1080/01614940.2014.946848

Smith, J. M. (Joseph M., Van Ness, H. C. (Hendrick C.), Abbott, M. M., & Swihart, M. T. (Mark T. (n.d.). *Introduction to chemical engineering thermodynamics*.

Sundaram, K. M., & Froment, G. F. (n.d.). *MODELING OF THERMAL CRACKING KINETICS-II CRACKING OF zso-BUTANE, OF n-BUTANE AND OF MIXTURES ETHANE-PROPANE-n-BUTANE*.

Tomishige, K., Asadullah, M., & Kunimori, K. (2004). Syngas production by biomass gasification using Rh/CeO2/SiO 2 catalysts and fluidized bed reactor. *Catalysis Today*, *89*(4), 389–403. https://doi.org/10.1016/j.cattod.2004.01.002

Vassilatos, V., Taralas, G., Sjöström, K., & Björnbom, E. (1992). Catalytic cracking of tar in biomass pyrolysis gas in the presence of calcined dolomite. In *The Canadian Journal of Chemical Engineering* (Vol. 70, Issue 5, pp. 1008–1013). https://doi.org/10.1002/cjce.5450700524

Wang, D., Czernik, S., Montané, D., Mann, M., & Chornet, E. (1997). *Biomass to Hydrogen via Fast Pyrolysis and Catalytic Steam Reforming of the Pyrolysis Oil or Its Fractions*. https://pubs.acs.org/sharingguidelines

Wang, L., Li, N., Lu, Y., Zhang, R., Sun, Z., Niu, S., & Luo, Y. (2022). Product distribution from pyrolysis of large biomass particle: Effects of intraparticle secondary reactions. *Fuel*, *325*. https://doi.org/10.1016/j.fuel.2022.124851
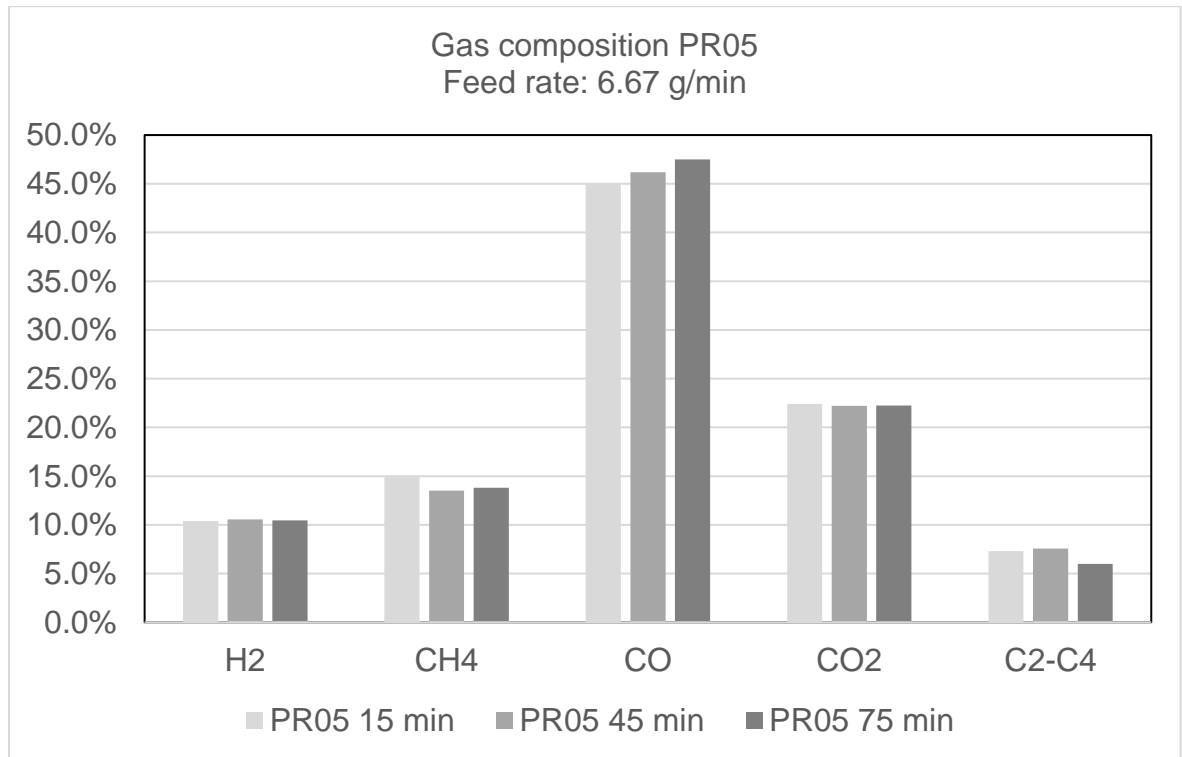
Wu, C., & Liu, R. (2010). Carbon deposition behavior in steam reforming of bio-oil model compound for hydrogen production. *International Journal of Hydrogen Energy*, *35*(14), 7386–7398. https://doi.org/10.1016/j.ijhydene.2010.04.166
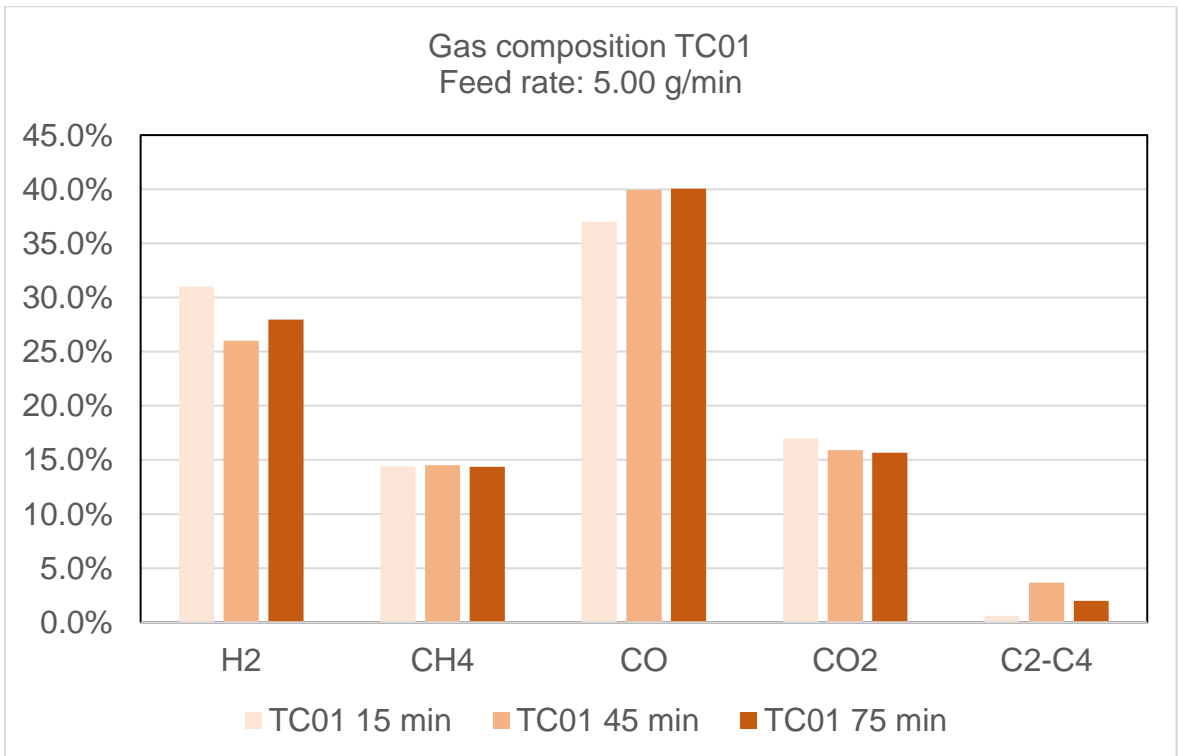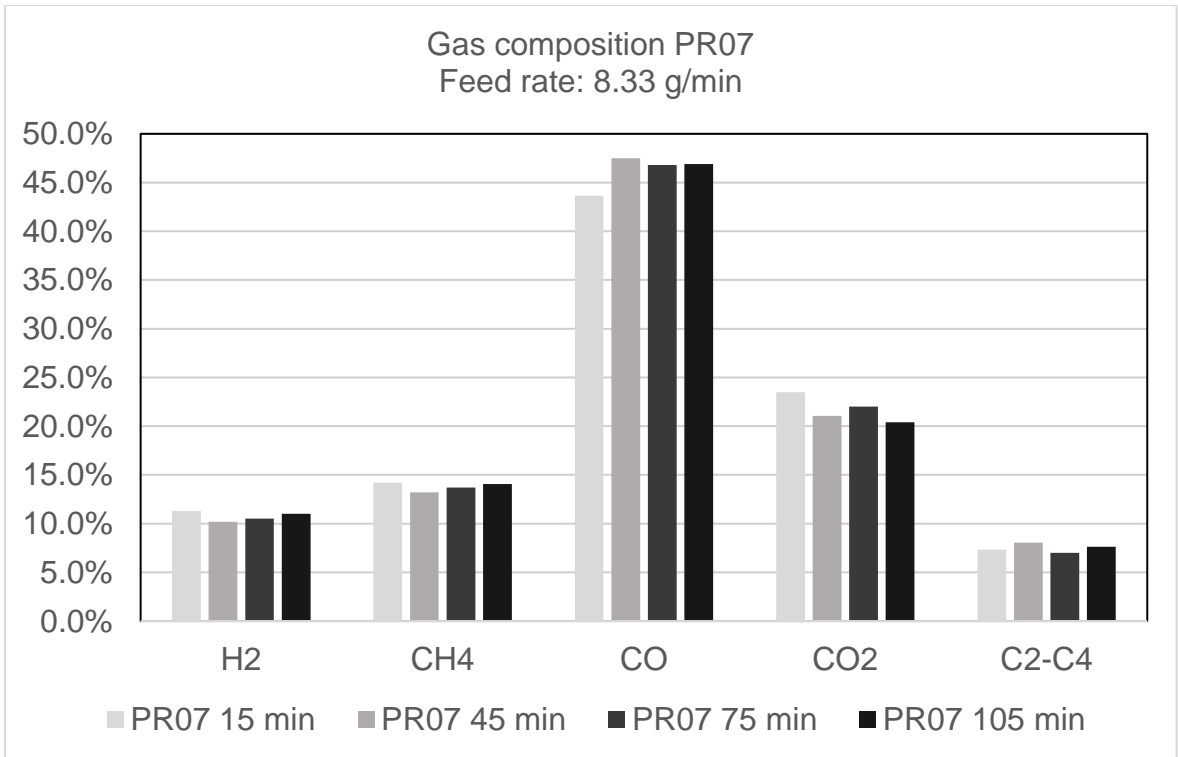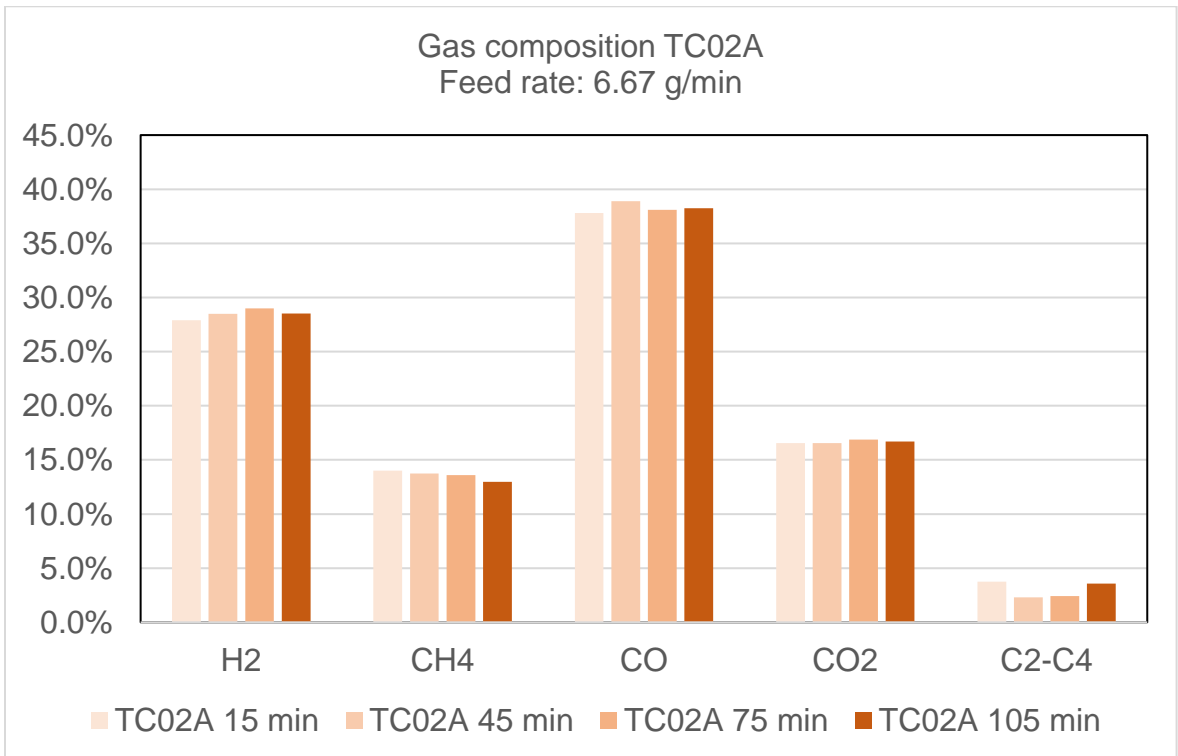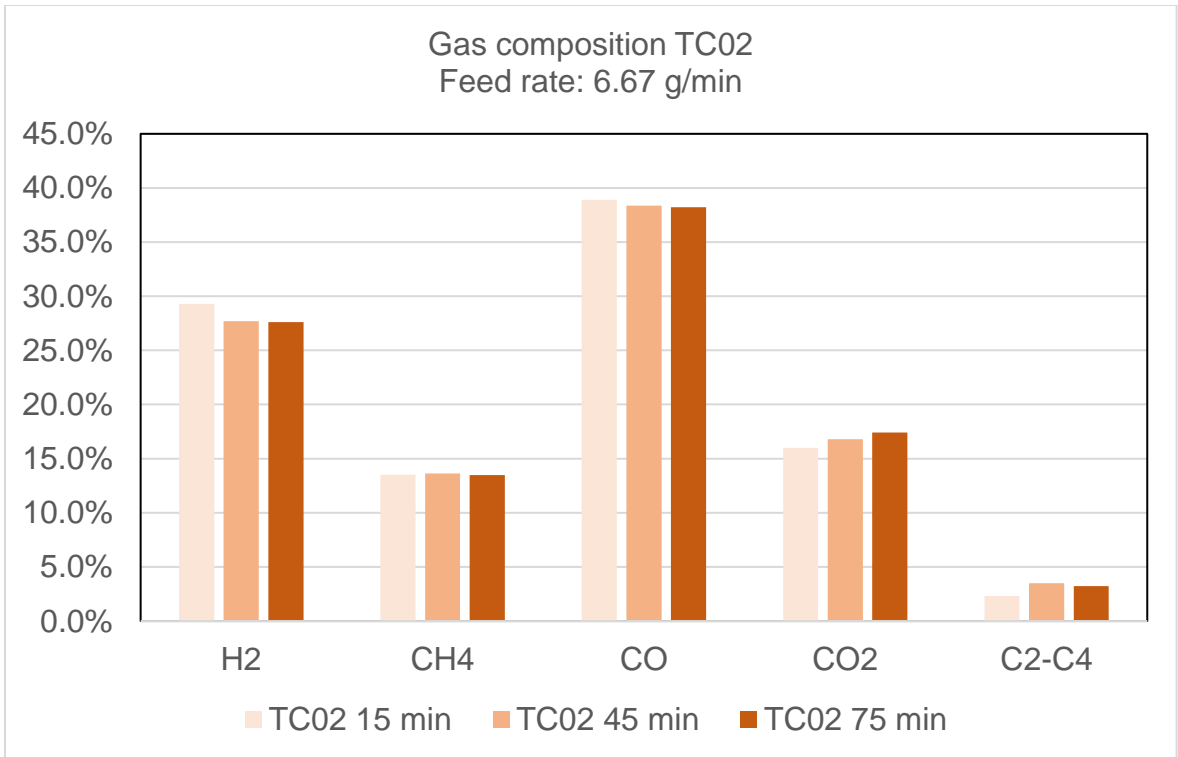
Appendices

Graphs of gas composition as a function of time for selected experiments

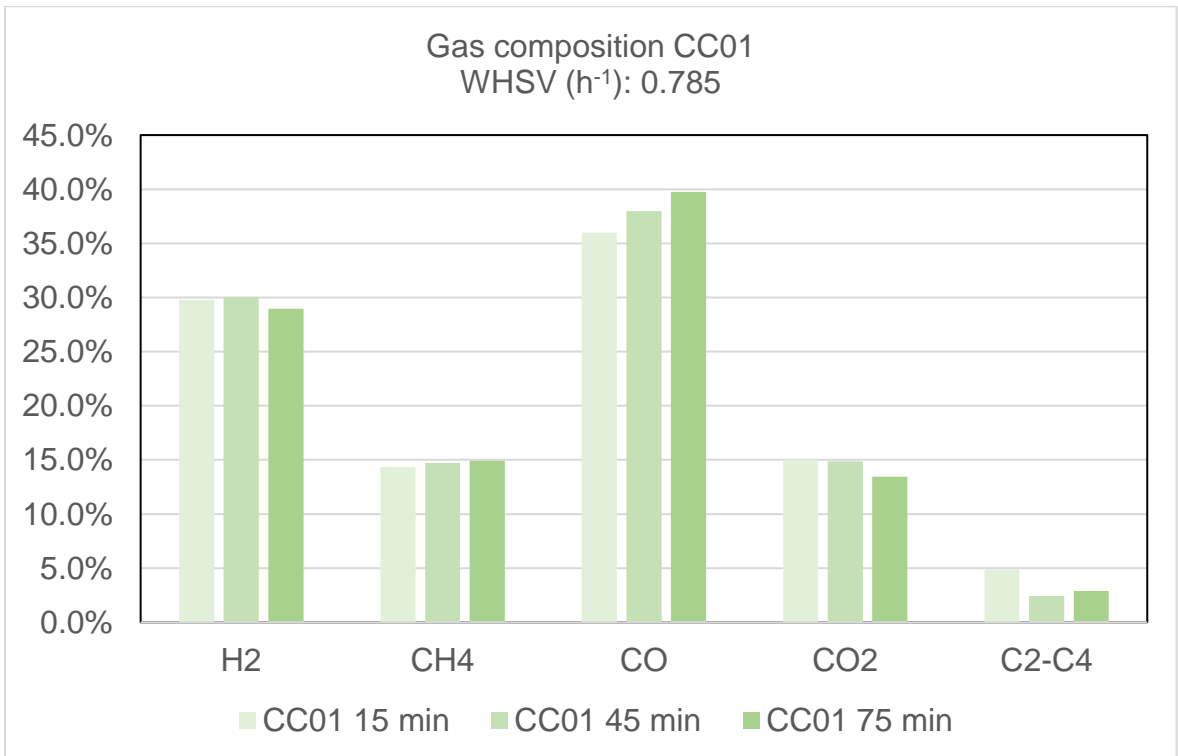All pyrolysis experiments carried out at 625 ^{o}C and 1 psig as operational conditions
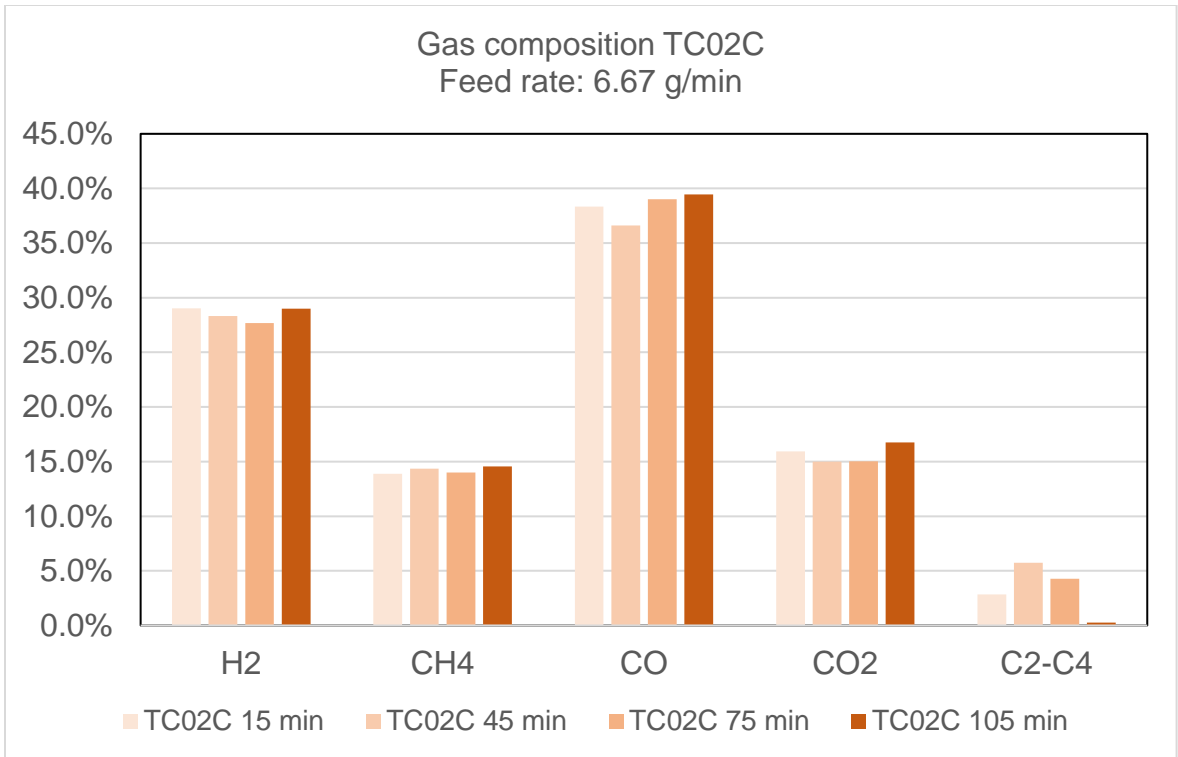
All thermal cracking (TC), catalytic cracking (CC) and catalytic steaming (CS) experiments carried out at 950 ^{o}C and 1 psig as operational conditions in second stage, and pyrolysis at same operational conditions mentioned above
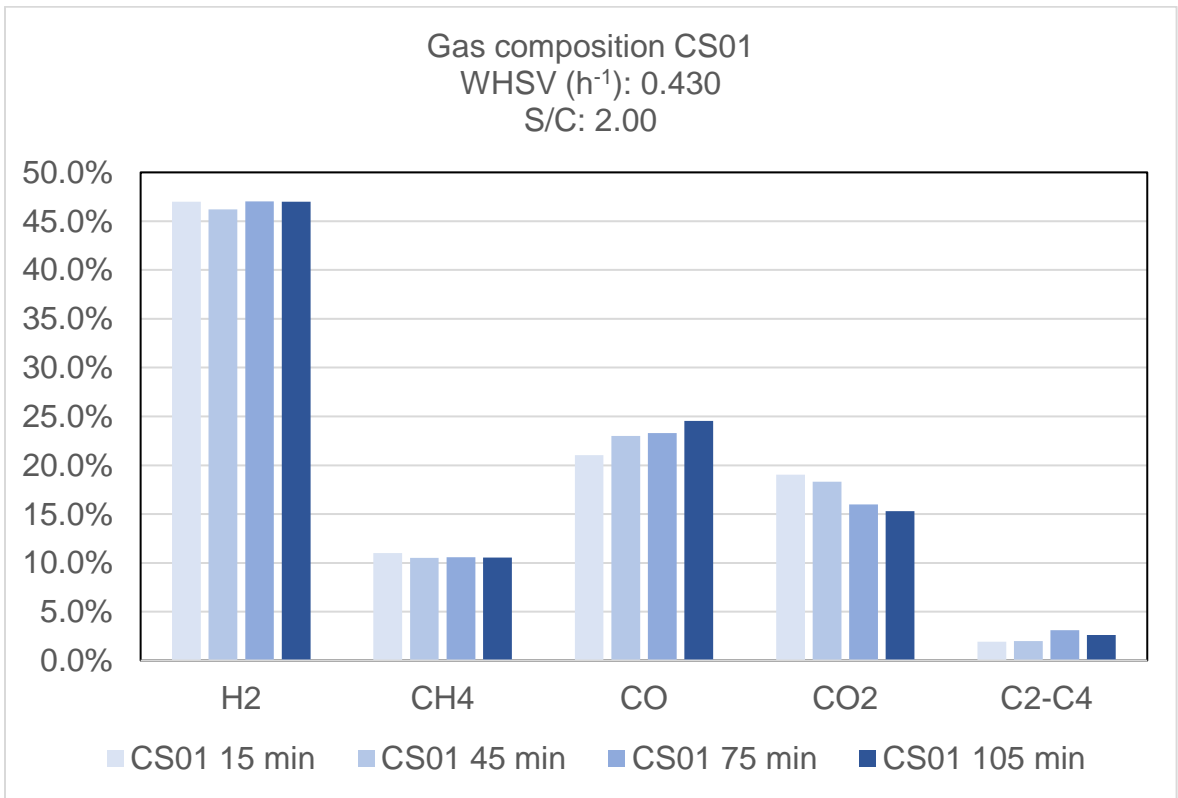

Gas composition PR05
Feed rate: 6.67 g/min

Gas composition PR07
Feed rate: 8.33 g/min

Gas composition TC01
Feed rate: 5.00 g/min

Gas composition TC02
Feed rate: 6.67 g/min

Gas composition TC02A
Feed rate: 6.67 g/min

Gas composition TC02C
Feed rate: 6.67 g/min

Gas composition CC01
WHSV (h⁻¹): 0.785

Gas composition CC05
WHSV (h^{-1}): 0.146

Gas composition CS01
WHSV (h^{-1}): 0.430
S/C: 2.00
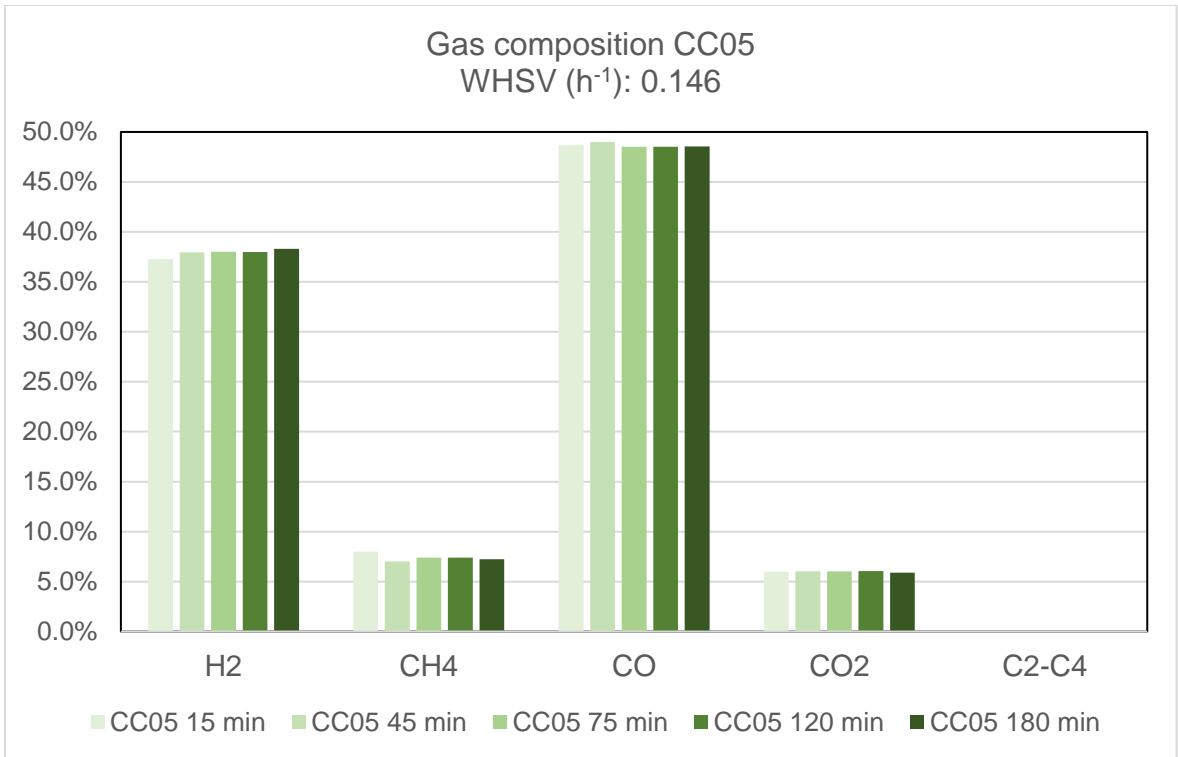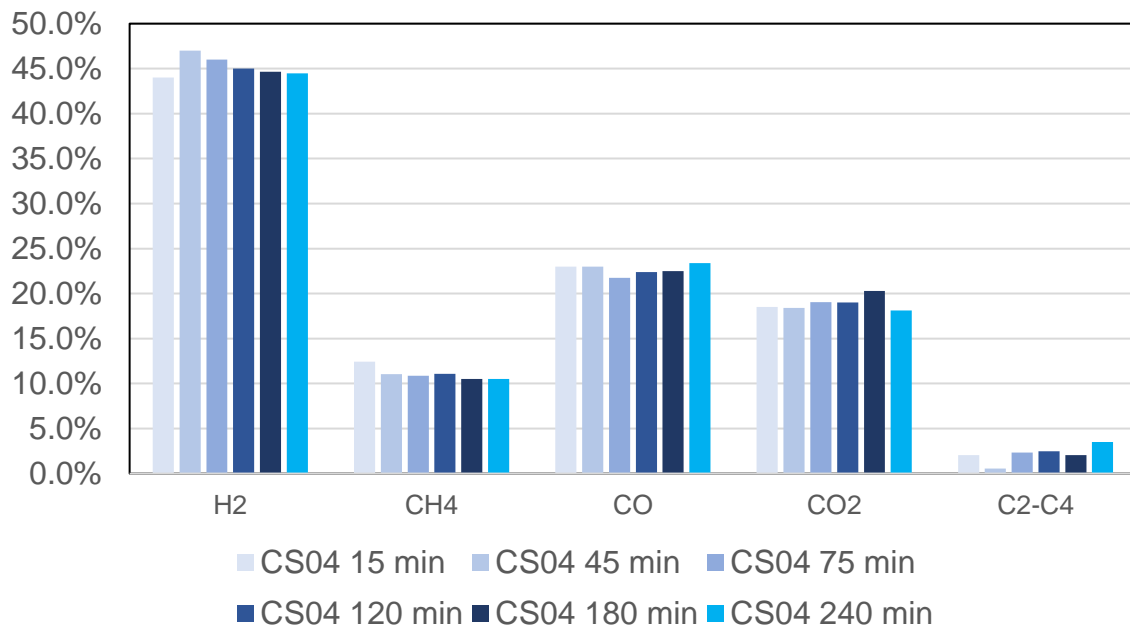
Gas composition CS04
WHSV (h⁻¹): 0.154
S/C: 1.60

Curriculum Vitae

Name: Ivan David Santiago Cespedes

Undergraduate: B.Sc. Chemical Engineering. EAN University

Bogota, Colombia

2015-2018

Awards: 100K for Americas. University of Texas San Antonio.

San Antonio, TX. USA

2017

Professional Experience: Part time professor. INCCA University

Bogota, Colombia

2019-2021

Part time professor. EAN University

Bogota, Colombia

2020-2021

Plant Manager. Leader Industries

Bogota, Colombia

2018-2020